Aravind Ramesh Chandran

Analysis of core losses in induction machine due to skewing

School of Electrical Engineering

Thesis submitted for examination for the degree of Master of Science in Technology.

Espoo 11.03.2013

Thesis supervisor:

Prof. Antero Arkkio

Thesis advisor:

Paavo Rasilo, D.Sc. (Tech.)

Aalto University
School of Electrical
Engineering

AALTO UNIVERSITY
SCHOOL OF ELECTRICAL ENGINEERING

ABSTRACT OF THE
MASTER'S THESIS

Author: Aravind Ramesh Chandran

Title: Analysis of core losses in induction machine due to skewing

Date: 11.03.2013 Language: English Number of pages:5+50

Department of Electrical Engineering and Automation

Professorship: Electromechanics Code: S-17

Supervisor: Prof. Antero Arkkio

Advisor: Paavo Rasilo, D.Sc. (Tech.)

This thesis deals with the analysis of losses due to skewing in induction machines. Normally skewing is done in induction machines to reduce noise, torque ripples and selective harmonics on the rotor cage of the machine. Skewing also can increase the effect of inter-bar currents in the machine. Due to die casting of rotor bars in the rotor at high temperatures, a very low resistance path develops between rotor bars. This resistance is called inter-bar resistance. Skewing is believed to promote these inter-bar currents and increase the stray losses happening in an induction machine.

The work was carried out using both measurements as well as simulations using finite element analysis. Two rotors were available at the Laboratory, one a skewed and another non-skewed rotor for a 37 kW induction machine. Locked rotor measurements were done by using both the rotors and the losses were calculated. Comprehensive measurements were done by changing different parameters such as frequency, torque, flux and current. A magnetic equivalent circuit and a multi-slice FEM model were also used to validate the results from the skewed machine. A small inter-bar resistance measurement set-up was also made. In the end all the data from both measurements and simulations were analysed and conclusions were drawn.

Keywords: Skewing, FEM, Inter-bar current, Inter-bar resistance

Acknowledgment

This thesis work was carried out at Aalto University, Finland in the department of Electrical Engineering under Prof. Antero Arkkio. I would like to thank first Prof. Arkkio for giving me this opportunity to work under him and do this research. As I was very new to this field, I am very much indebted to Paavo Rasilo my supervisor, who guided me through each and every step of this thesis. Those brainstorming sessions for getting new ideas and moving into the right direction helped me a lot to finish this thesis.

There were lot of measurement setups in this work which wouldn't have been possible without Ari Haavisto, who guided encouraged and discussed with me in building up each of the set up's successfully. I would also like to thank Prof. Anouar Belachen for helping me in clarifications of my research methodology and guiding me forward. I would always cherish the moments with my colleagues at the department of Electromechanics at Aalto university for providing me with a good work environment and supporting me for my thesis. The contribution from the side of my friends at Aalto who helped me and supporting me were immense and I am grateful to them for that.

Finally I would like to thank my parents for helping me grow up and helping to do all these. The final writing stages of my thesis were full of hardships and tested me to my capabilities. I thank the almighty for giving me strength for not giving up and finish this thesis.

Otaniemi, March 27, 2014

Aravind Ramesh Chandran

Contents

Symbols and abbreviations

Symbols

μ:	Permeability of the reluctance element
A:	Area of the cross section along which the flux flows
dx:	Elementary section of the rotor axially
f_1	Stator frequency
g	Contact conductivity per unit length
h	Electrotechnical iron sheet conductivity per unit length
f_2	Rotor frequency
I_1	Stator current
I_2	Rotor current
K_d	Winding factor
K_skew	Skewing factor
len:	Length of the reluctance element along which the flux flows
l:	Rotor length
L_ers	Inductance of the end winding
m	Number of phases
n_r	Synchronous speed
n_s	Rotor speed
p	Pole pairs
P_input	Input power
P_losses	Total Losses in the machine
P_mech	Mechanical output power of the machine
r	Bar resistivity per unit length
R_1	Stator side equivalent resistance
R_2	Rotor side equivalent resistance
Rel	Reluctance
R_ers	Resistance of the end winding
s	Shaft resistivity
X_1	Stator side equivalent leakage reactance
X_2	Rotor side equivalent leakage reactance
X_m	Magnetizing reactance

Abbreviations

FCSMEK	FEM tool for analysing electric machines developed at the Laboratory of Electro-mechanics at Aalto university
FEM	Finite element method
FORTRAN	General purpose imperative programming language mostly suitable for numerical calculations
GPIB	General purpose interface bus
MEC	Magnetic equivalent circuit
mmf	Magnetomotive force

1 Introduction

1.1 Motivation

The amount of electrical energy consumed by rotating machines comes at around 50% of the total power produced around the world. With all the losses in the transmission and distribution network, the amount of power required to be generated at the power utility are far high. So a small change in the efficiency of an electric machine would mean valuable savings in the energy production. The determination of losses in electric machines and tweaking the design of a machine to achieve more efficiency has been a great challenge to mankind in the last century. Induction machines are known for their ruggedness, reliability and ease in manufacturing. This makes them more suitable for industries in constant speed application. With the advent of power electronics, nowadays they have been used in variable speed applications also. So a minor tweak in the efficiency of an induction machine would lead to major savings of power.

1.2 Aim

Of all the losses, reduction of stray losses in induction machine has been an interesting topic to play with. Studies show that skewing the rotor of an induction machine has changed the stray losses and also the performance of the machine. This change in losses can be due to the inter-bar currents in the rotor, due to imperfect insulations between bars and insulations and also elimination of certain space harmonics in the air-gap. This thesis aims at the analysis of the effects of skewing on the losses in an induction machine. Measurements would be done to a 37 kW induction machine, with a skewed and a non-skewed rotor analysing the differences in losses. Multi-slice finite element models would be used to validate and analyse the results.

1.3 Thesis outline

The uncertainty of the problem makes the choice of measurements and analysis to be done, hard to choose. Results from the preceding analysis would lead to insights on what have to be done further. The thesis is also written in a similar pattern as how each step has been carried out in this analysis

Second Chapter This chapter deals with the previous work done on the topic and little bit of basics so that the reader can understand the rest of the chapters.

Third Chapter The third chapter deals with how the problems were approached and what decisions were taken on getting results from each analysis.

Fourth Chapter This chapter explains the magnetic equivalent circuit used in the analysis and the comparison made with it.

Fifth Chapter This chapter explains and analyses all the comprehensive measurements made during the thesis and there results.

Sixth Chapter All the final discussions and conclusions are drawn in this section.

2 Theory

2.1 Induction machines

Induction machines are considered to be very important for the industries today with there ruggedness and cheap manufacturing process. The induction machine or the asynchronous machine consists of a stator and a rotor. The stator of the induction machine has mostly distributed winding, similar to those in synchronous machines. The windings are distributed into poles and phases. Each phase winding in the machine is displaced by 120° and the three phases in the winding creates a sinusoidally distributed mmf wave centered on the axis of the coil. The mmf produced from the 3 phases makes a resulting rotating mmf along the air-gap. This rotating mmf creates a rotating magnetic field which is also sinusoidal in the air-gap due to the arrangement of the windings. The speed of the rotating field referred to as synchronous speed (n_s) is proportional to the frequency of the current source fed to the stator.

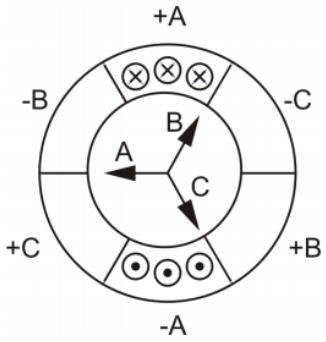

Figure 2.1: MMF in each phase;[1]

The rotor of an induction machine, often referred as a squirrel cage is generally a cage with copper or aluminium bars shorted with endrings. This forms the basis for the working of an induction machine. The rotating magnetic field in the air-gap cuts the stand still rotor bars and induces currents in them. The rotor bars acts like current carrying conductors in a magnetic field and hence forces acts on them resulting in torque production of the machine.

The torque produced rotates the rotor at the rotor speed (n_r) to near synchronous speed and not the synchronous speed, because at this speed the relative speed between the rotor and the rotating magnetic field becomes zero and the current induced

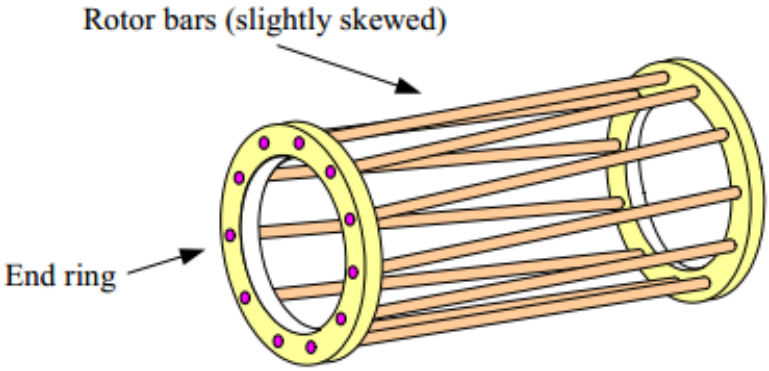

Figure 2.2: Rotor cage;[1]

in the rotor becomes zero and hence no force is produced. The relative difference between the rotor speed and the synchronous speed is termed as slip (s).

$$s = \frac{n_\mathrm{s} - n_\mathrm{r}}{n_\mathrm{s}} \tag{2.1}$$

As the rotor speed approaches the synchronous speed the rate at which the the flux linkage cutting the rotor bars of the rotor decreases, hence the current induced on the bars also reduces. The frequency of the rotor current could be represented as:

$$f_2 = s \cdot f_1 \tag{2.2}$$

2.2 Equivalent circuit representation

An analytical model for an induction machine can be formulated using an equivalent circuit.This model is often called as a "Transformer model", because an induction machine could be attributed to a rotating transformer with the secondary shorted.

From the equivalent circuit one could write the following equations:

$$P_\mathrm{Input} = 3I_1^2 R_1 + 3I_2^2 \frac{R_2}{s} \tag{2.3}$$

$$P_\mathrm{Losses} = 3I_1^2 R_1 + 3I_2^2 R_2 \tag{2.4}$$

$$P_\mathrm{Mech} = 3I_2^2 \frac{R_2}{s}(1 - s) \tag{2.5}$$

The effect of core losses can be taken into account by adding a resistance in parallel to the magnetizing reactance X_m. The effect of friction and windage are subtracted from the output power. With the help of the above equations, the efficiency of

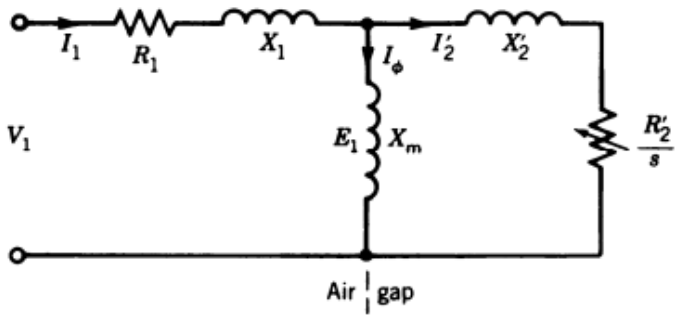

Figure 2.3: Induction motor equivalent circuit;[1]

the machine could be predetermined. While comparing this value of efficiency to the measured efficiency, there is always a change of 2-3% under loaded conditions. These extra losses could be termed as stray losses. Based on the studies in the paper [2], the contributions of stray load losses can be attributed to surface losses due to harmonics, rotor inter-bar currents, pulsation losses, high-frequency losses and leakage flux losses.

One of the main reasons for noises in an induction machine is due to the interaction of stator and rotor harmonic fields. The harmonics of the stator field induces voltage in the rotor, and hence these rotor currents produce several harmonics in the rotor mmf. The 5th and 7th harmonics produce asynchronous torque in the machine, which produces a negative effect in the production of the torque of machine. During the design phase of the winding, care is taken that the amplitude of the 5th and 7th harmonics are reduced through methods like chording and selection of appropriate number of slots. Harmonics of the order m(number of phases) and p(number of pole pairs) are always higher than the other harmonics present in the machine. Many of these could be avoided by skewing the machine, thereby reducing the coupling between the rotor and the stator harmonics. Skewing significantly has an impact on the stray losses.

2.3 Skewing in induction machine

Skewing is normally done in small machine, to avoid the effect of slot harmonics in the machine, hence reducing losses. This could reduce the effect of high frequency ripple and other acoustic noises in the machine. Skewing is not done in large machines, because most of the time they are not made by die casting, where such a technique would make the manufacturing difficult. It also improves the torque-speed characteristics of a machine, since to an extent it eliminates all the asynchronous torques produced. Although skewing reduces the losses due to the harmonics induced in the rotor cage due to stator slotting, there are other effects which could prove otherwise. Skewing introduces inter-bar currents in the rotor due to imperfect insulations between rotor bars. It also introduces a change in axial flux density

distribution in the machine, which may increase the saturation in the machine and hence the losses.

The pull out torque which is the minimum torque produced in the torque speed characteristics is greatly influenced by the 5th and 7th harmonics produced. These torques are greatly influenced by the rotor impedance especially when the rotor frequencies are pretty high.The relation between inter bar resistance and die casting has been discussed in [3]. When the rotor bars are casted using copper, due to the high melting point of copper, the rotor stack lamination experiences a high temperature, this high temperature gives copper a good physical and electrical contact with electrical steel. This increases the chance of imperfect insulation between rotor bars, hence a path for inter-bar currents to flow through is created.

One of the approaches to consider the effect of skewing on the machine is by using the skewing factor. This factor is mostly used in all the analytical models of induction machines. Since skewing reduces the coupling between the stator and the rotor, it reduces the induced voltage over the rotor from the stator. The effect of winding factor in the machine is also a reduction of induced voltage on the machine, thus the derivation of skewing factor of a machine could also be done in a similar way. The skewing factor could be derived from the winding factor (Eqn 2.6).

$$k_{\mathrm{d}} = \frac{sin(vq\frac{\alpha}{2})}{qsin(v\frac{\alpha}{2})} \tag{2.6}$$

Considering the skewed bar to be a finite number of short bars, at different angles as shown in the Fig 2.4.

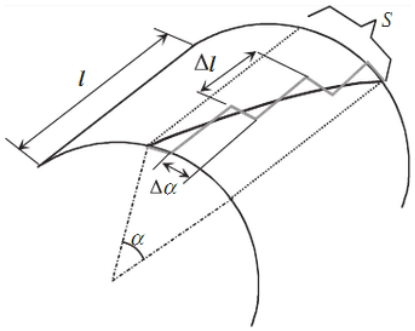

Figure 2.4: Deriving skewing factor;[4]

The number of such small bars can be written as :

$$z = \frac{l}{\Delta \cdot l} = \frac{\alpha}{\Delta \cdot \alpha} \tag{2.7}$$

Putting the value of z from Eqn. 2.7 to q in Eqn 2.4 and assuming the angle $\Delta\alpha$ to be very small, we get the value for skewing factor as

$$k_{\text{skew}} = \frac{sin(v.\frac{\alpha}{2})}{v \cdot \frac{\alpha}{2}} \tag{2.8}$$

This expression could be multiplied at the same place where the winding factor is included to get the resulting induced voltage in the machine. The text [4] clearly explains the elimination of slotting harmonics, on choosing proper value of skew (1 stator slot pitch) in the machine.

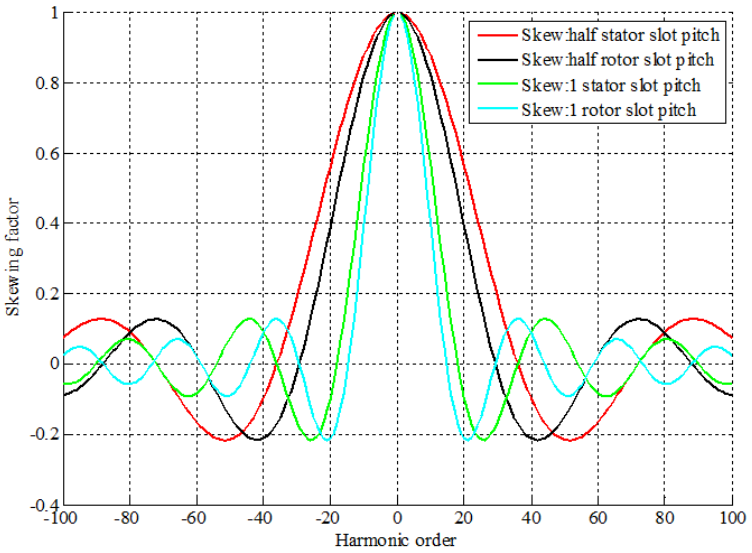

Figure 2.5: Skewing factor verses harmonic order

Fig 2.5 shows that when the rotor of an induction machine is skewed by one stator slot pitch, there is significant reduction in the orders $\pm 19, \pm 17, \pm 35$ which are the slotting harmonics of the machine. So proper selection of skewing could eliminate selected harmonics as needed in a specific application.

2.4 Inter-bar currents

The phenomenon of inter-bar currents has been explained very nicely by the author of [5]. The basic principle of Lenz's law could be used to explain the principle of inter-bar currents. The Fig 2.6 shows 3 types of rotors: (a) shows an ideal skewed rotor with perfect insulation between the bars. The time-varying flux induces a current in the rotor bars which loops around the bars. (b) shows a practical rotor with some imperfect insulation between the rotor bars, in which localized current loops are formed which flow between the bars increasing the losses. (c) shows a non-skewed rotor where the inter-bar currents are cancelled with the two adjacent localized current loops.

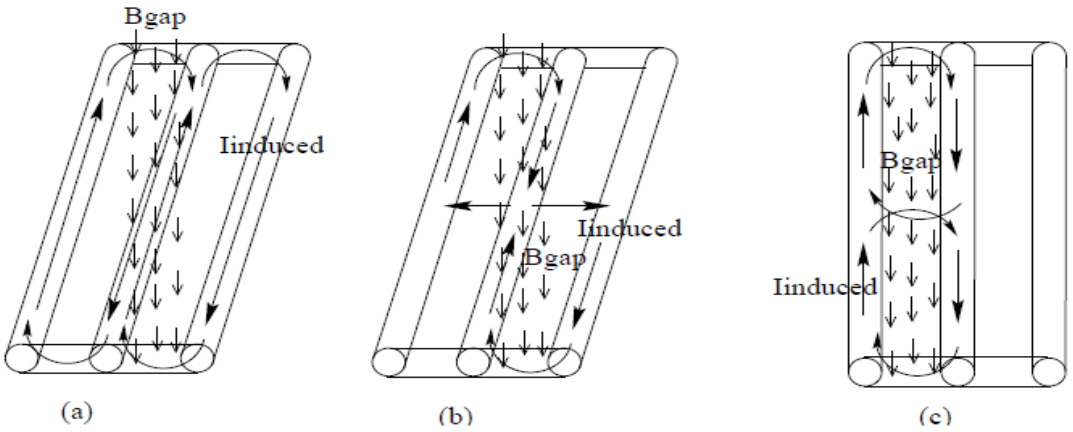

Figure 2.6: Origin of inter-bar currents;[5]

2.5 Previous studies

Research on stray load losses in induction machines have been studied by Odok in 1958 [6]. He has discussed about experiments to measure inter-bar resistance. He has also discussed about voltage and current induced in the rotor bar due to harmonics arising from the stator on a skewed induction machine. Based on this paper Dabala has discussed quite a few methods to determine rotor bar-iron resistances in his paper [7]. Here he categorizes them into destructive and non-destructive type of measurements.

In a more recent study conducted by Stening in his work [8], he has made a test set up for inter-bar resistance measurement. Deriving from this he has made an analytical model for inter-bar currents. He points out from his measurements that the inter-bar resistivity is lower in cast of copper rotor than in the cast of aluminium rotors.

Another study related to inter-bar currents was discussed by Englebretson in his paper [5]. The author has discussed the effect of inter-bar current, and has added the effect of inter-bar currents onto the equivalent circuit. He also suggests the use of insulated rotor bars to eliminate the effect of inter-bar currents. Skewing the rotor in the other axial direction would have no effect on the performance of the machine. The flux in the air-gap and the emf induced onto the rotor cage would be same for a negatively skewed machine. Yet identical rotors with the same amount of skewing can have different performance and stray load losses. This can be due to manufacturing error as well as change in the inter-bar resistance due to the casting process.

Williamson and Smith analyses locked measurements for 5 identical machines with the same skew in [9]. These results gave different values of locked rotor torque, which infers different values of rotor resistance. This change in rotor resistance may indicate different temperature during locked rotor measurements or different

inter-bar resistance during die-casting.

The effects of skewing on losses have been discussed in the paper [10]. The author explains the variation in losses due to skewing in the following manner. The resulting air gap mmf in a machine is due to the interaction between the stator mmf and the rotor MMF. Skewing changes the phase of the rotor mmf to the stator mmf axially, and this leads to a change in flux distribution along the length of the machine. The air gap flux at one end of the machine is higher than other, so the saturation would also change axially in the machine. So this is why skewing can alter the losses in machine. Since saturation is a non-linear phenomenon, the increase in losses in one side of the machine due to saturation wont necessarily cancel out the decrease in losses on the other side. Since skewing reduces the coupling between the stator and the rotor, this adds an additional leakage reactance component to the machine.

The author also says about the effect of skewing on rotor joule losses. Skewing is found to decrease the high frequency currents induced on the rotor bars due to stator slotting, hence reducing the rotor joule losses. But these induced currents in the rotor bar were helping in damping the stator slotting harmonic fields; this increases the iron losses in the machine. So the amount of skewing in the machine determines the balance between rotor joule losses and rotor iron losses. So the total losses could be balanced, which could make the losses unchanged, provided that there is no saturation. If there is saturation, the process becomes non linear. The author explains that the effect of skewing varies for big machines and small machines. If the specific electric and magnetic loading of the machine are kept constant, Then the copper loss in a machine is proportional to the air gap diameter and the iron losses in a machine is proportional to the square of the air gap diameter. So for smaller machines, the amount of copper loss is higher than the iron losses, so skewing would reduce the total losses in the machine. But in large machines, the amount of iron losses are higher, so skewing would increase the iron loss even more hence skewing would not prove beneficial.

3 Research methodology

The problem at hand was analysed through various measurements. The machine available in the lab for analysis was a 37 kW induction machine stator housing, with an option of two rotors. Rotor A was a skewed rotor, while rotor B was a non-skewed rotor. Since the main topic of interest is skewing and its influence on inter-bar currents, the simplest way to go forward would be due to a locked rotor test, so that maximum current flows through the rotor bars and the effect of the inter-bar currents could be magnified.

While measurements are the reference to all the analysis, simulations play an important role and help to predict the behaviour of the machine and mostly direct the analysis to a positive direction. With the available parallel clusters of computing power, finite element analysis is one of the best numerical methods that could predict the behaviour of an electric machine. In this work Finite Element Method(FEM) has been used widely for checking the plausibility of the measurements and results from analytical models. FEM results have also been used to point the direction of the analysis.

3.1 Finite element analysis

The conventional analytical models for an induction machines are designed to give results based on the approximate value of flux density inside the machine, such methods would lead to good results in steady state operations. But in order to determine the change in the minor losses that happens inside the machine, FEM has proven to be a plausible method with the current status of processing powers available. On the grounds of electric machines, basics steps involved inside FEM have been explained below for the understanding of a layman. Basically FEM has three stages:

- Model creation: The geometry of the electric machine under analysis is made and subdivided into discrete or finite elements. The geometry is often a 2d or 3d model. The resulting geometry that you get after performing the subdivision is often referred to as a mesh. Size of the mesh is mostly chosen based on the computation time and the level of accuracy needed in the model.

- Analysis: Using Maxwell's equations, differential equations are formulated. Enforcing boundary conditions to these equations in the mesh and solving them using numerical methods like the Galerkin's method would yield solutions from which results could be interpolated from each and every point over the mesh.

- Post processing: In this stage, the solutions from the above steps are graphically displayed on the mesh, so as to identify the hotspots and other important parameters from the model.

The finite element program used was FCSMEK which was developed at the Laboratory of Electromechanics of Helsinki University of Technology. This program is

developed from FORTRAN and can be used for the analysis of both induction machines as well as synchronous machines. FCSMEK has already defined templates, which contains the flexibility of choosing the slot shape and the dimensions of the machine.

Usually FEM for radial flux electric machines is modelled in 2d which requires less computational time than a 3d model. They are widely used in all kind of electrical machines ranging from permanent magnet machines to induction machines. Depending upon the number of the slots of the stator and the rotor as well as the pole pairs of the machine, the FEM simulations could be performed on a partial geometry thus reducing the time of computation. A simple 2d mesh for an induction machine can be represented from the following figure.

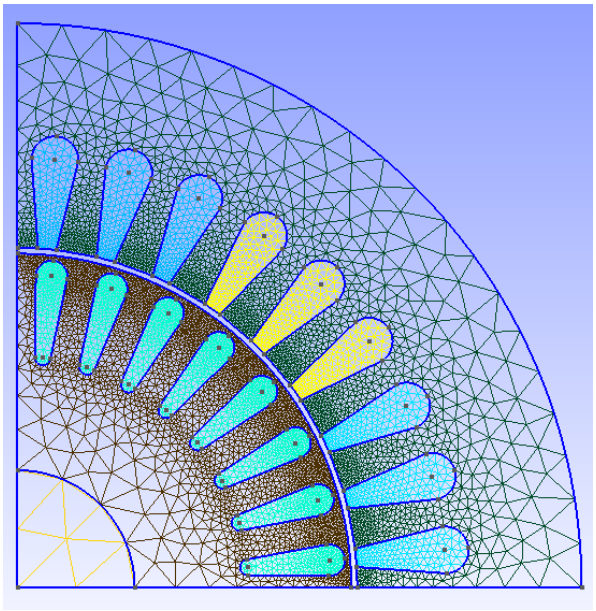

Figure 3.1: Finite element mesh for an induction machine;[11]

Fig 3.1 shows the mesh for an induction machine where the symmetry of the machine has been exploited for faster calculation of the solution. Since skewing is a property which can be represented only with a 3-d model, multi-slice models could be employed to consider the effect of skew in the machine. FEM was extensively used in this work and simulations were carried out for different operating points and conditions, so that we can analyse the changes in losses due to skewing.

3.2 Analysis of rotor losses with different rotor positions using FEM

To check whether if the position of the rotor has any influence on the losses during the locked rotor test; FEM simulations were carried out with different rotor position and the rotor losses were analysed. As already mentioned, the machine under analysis is a 37 kW induction machine with 40 rotor slots. The rotor slot

pitch would be $360\,^\circ/40\,^\circ = 9\,^\circ$. So the simulations were done with 10 rotor positions starting from $0\,^\circ$ to $9\,^\circ$.

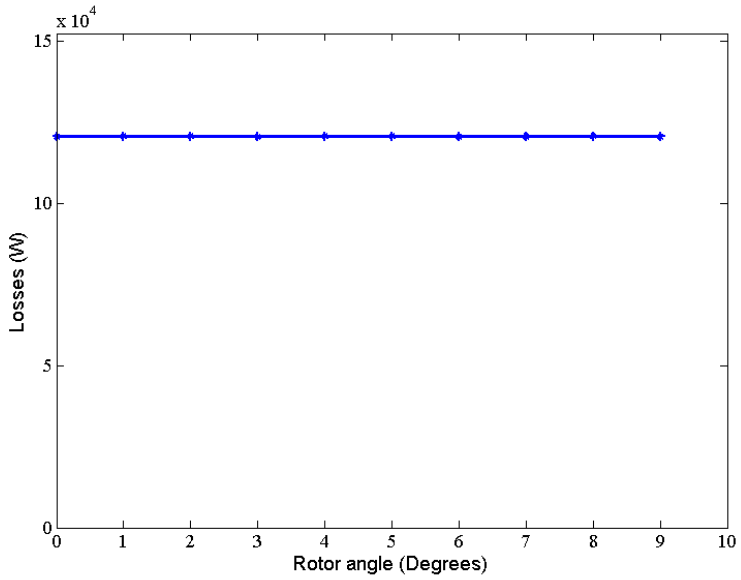

Figure 3.2: Total losses - stator resistive losses, plotted with different rotor angles

The data obtained from the FEM simulation shows that there are no considerable changes in losses by changing the position of the rotor. So similar measurements won't be done on a real machine.

3.3 Locked rotor test

Standard locked rotor measurements were done on the 37 kW induction machine. The measurements were carried out on the skewed as well as the non-skewed rotor. There are numerous options regarding the parameters to be kept constant in each measurement. Since the rotors are different, they would behave differently under different operating conditions. Before deciding all these parameters, the measurement set-up is explained in the following.

Measurement setup

The rotor shaft was blocked through a coupler blocked with a piece of iron rod. As shown in the figure, the iron rod rests over a weighing balance which shows how much force is exerted, and hence the torque could be computed. The length of the iron rod was 333 mm.

The machine was fed from a series of generators and motors. Inorder to avoid all the time harmonics from the supply, a rugged and reliable power source was needed so that only the space harmonics affected the losses in the machine. The arrangement is as shown in Figure 3.4.

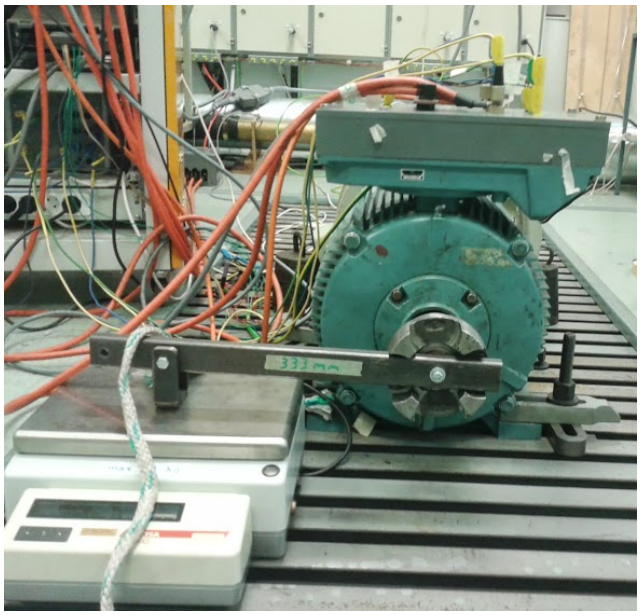

Figure 3.3: Locked rotor test setup

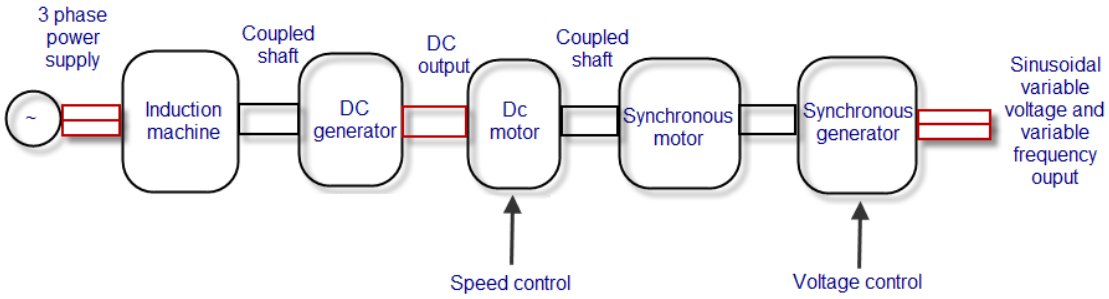

Figure 3.4: Sinusoidal variable voltage and variable frequency power source

All the measurements like voltage, current, power etc, where measured using NORMA D6100. The temperature measurements were done with thermocouples. They were installed at 5 parts of the machine, 4 of them were on the end-winding, and one of them was on the rotor which heated the most. Since the rotor is locked, large amount of current is induced in the rotor and it is essential to keep track of the temperature of the rotor. The temperature sensors are directly connected to a FLUKE Hydra. Both the FLUKE Hydra and the Norma are interfaced to Matlab from which the data can be evaluated through a GPIB cable.

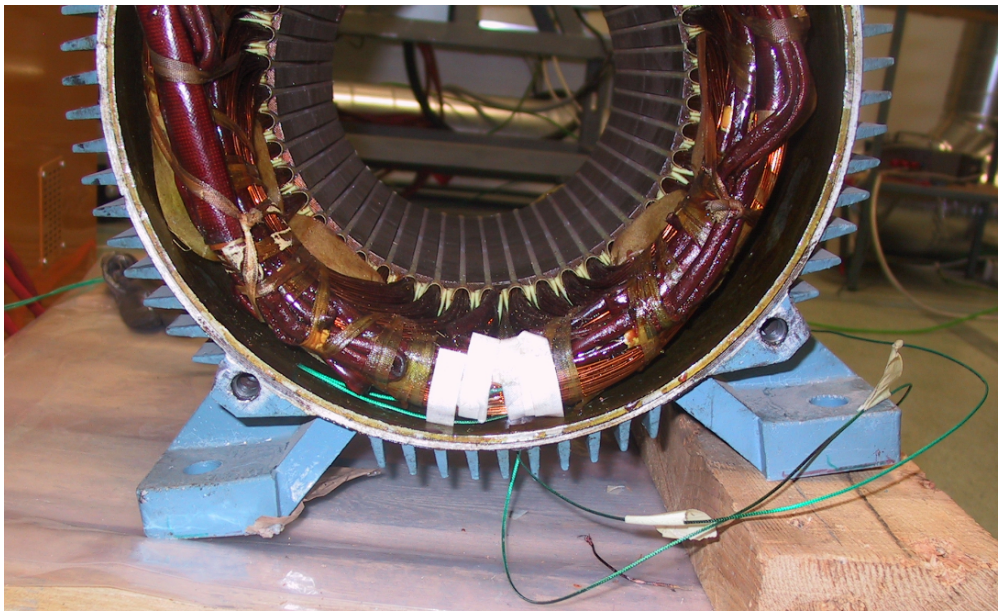

Figure 3.5: Temperature sensor installed on the stator end winding

Additional information that would be useful is the flux in the air-gap of the machine. This could be measured with the use of search coils, they were installed in the stator slots of the machine to measure flux in the air gap. Basically they are just coils wound inside the air-gap so that the flux linkage in the air-gap could induce voltage in them. Since the machine under consideration had 4 poles in the stator, 4 search coils were installed which started from the first slot in the stator to the 13th slot covering each pole. This could give information on the eccentricity of the rotor if the flux in the 4 poles were different. Since changing the rotor needs to be done in the experiment between a skewed and a non-skewed rotor, utmost care is required with respect to the placement of the search-coils so that they are not damaged while changing the rotors.

The measurements are to be recorded when the machine reaches a thermal equilibrium. Time is given for the system to stabilize the temperature as well as the losses. As per the standard [12], a thermal steady state is attained when there is no more than 1 °C variation in temperature when measured at two successive 30-minute intervals. The criteria set in this work is that Δ T $< 0.5\,^{\circ}$C in a period of 60 minutes. On an average it took around 6 hours for the machine to reach steady state. Resistance measurements of the stator windings were done by feeding a 5 V DC voltage source to the stator winding, simultaneously measuring the voltage and current in the circuit. Initially the cold resistance of the stator was recorded before the measurement was started. In the end when the machine reaches the thermal equilibrium, the machine would be turned of immediately and a cooling curve would be plotted using the DC measurement set-up. Again from the standard [12] the cooling curve could be plotted for a period of 30 seconds or more. From this curve the stator resistance at the instant of turn off was interpolated. An electro-mechanical switch was used to switch between the main supply and the DC supply

for the resistance measurements during switch-off so that we avoid any high currents flowing into the resistance measurement set-up. The measurements were done using FLUKE multi-meter interfaced to Matlab, where all the calculations were done.

3.4 Results with operating point as current

The first parameter that could be made constant between a skewed and a non-skewed rotor can be the stator current. So measurements were taken with current kept constant in each operating point. All the measurements were recorded after the machine had reached thermal equilibrium as discussed in the last section. The results for the measurements are shown below in Fig 3.6.

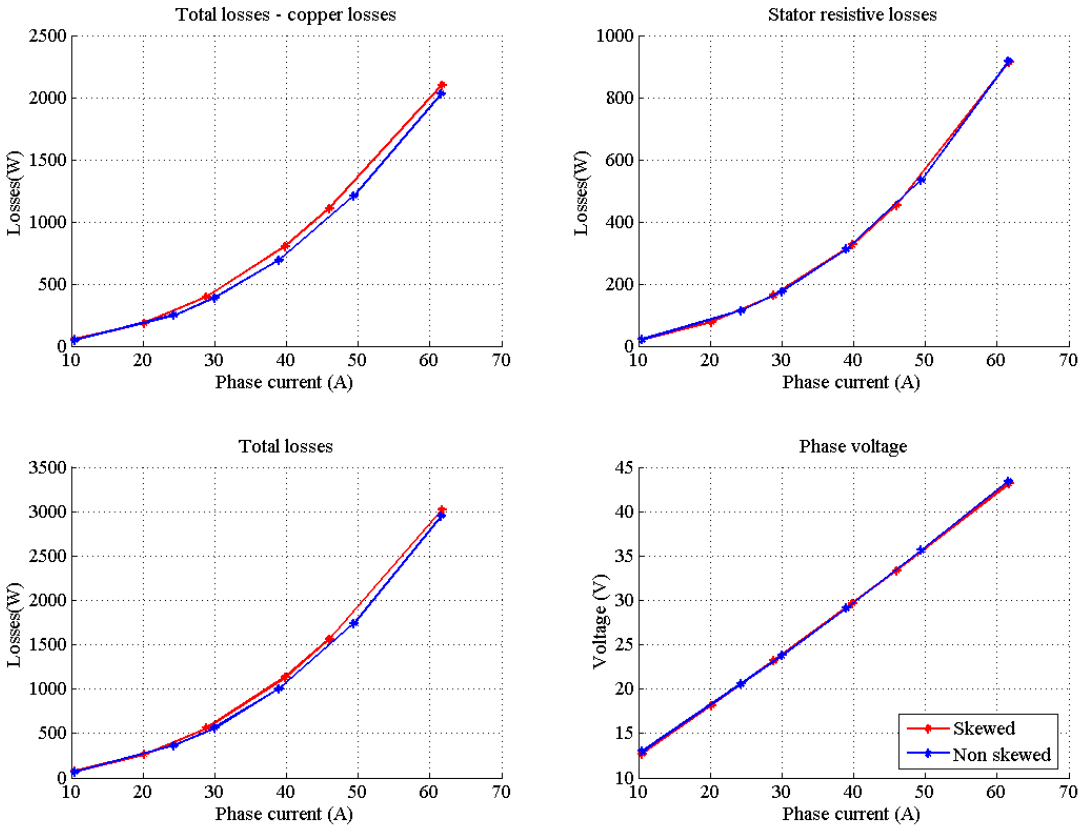

Figure 3.6: Comparison of rotor losses in both skewed and non skewed rotor

Since the operating points (stator currents) are kept constant for both the rotors, the resistive losses in the stator as seen from the results are found to be almost the same. The losses plotted above include rotor resistive losses, rotor core losses and stator core losses. There seems to be a slight change in the amount of losses between a skewed and a non-skewed rotor, which can be visualized more clearly in the Fig 3.7.

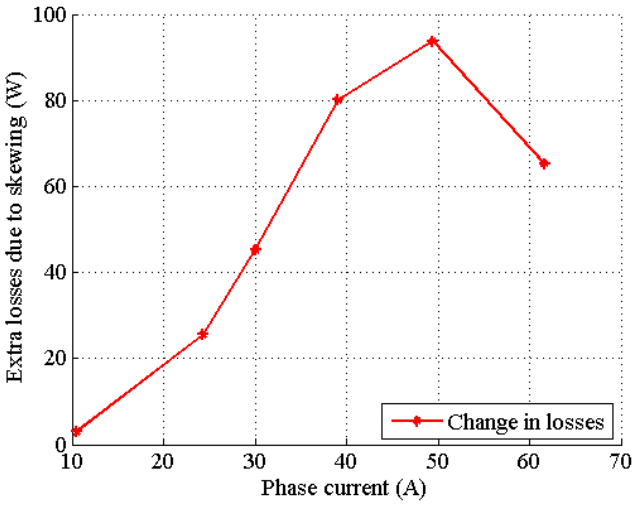

Figure 3.7: Increase in losses due to skewing

The torque measured also showed a difference that the non-skewed machine had a higher torque value than a skewed machine.

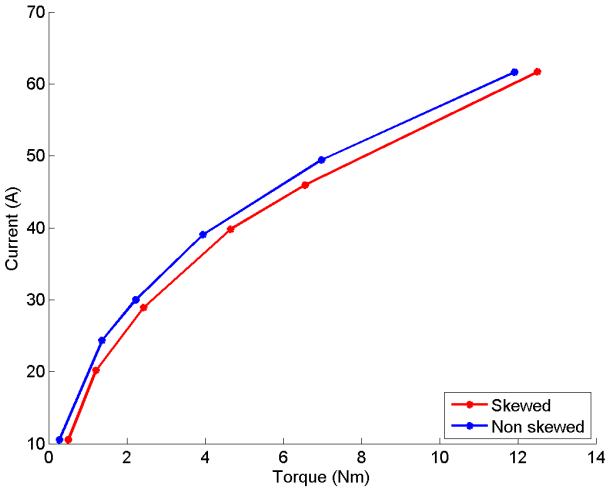

Figure 3.8: Change in the torque measured

3.5 Validation of the measurement with FEM for the non-skewed rotor

The measurements were now compared with the simulations using finite element analysis with the software fcsmek. The comparisons are shown in the Fig 3.9.

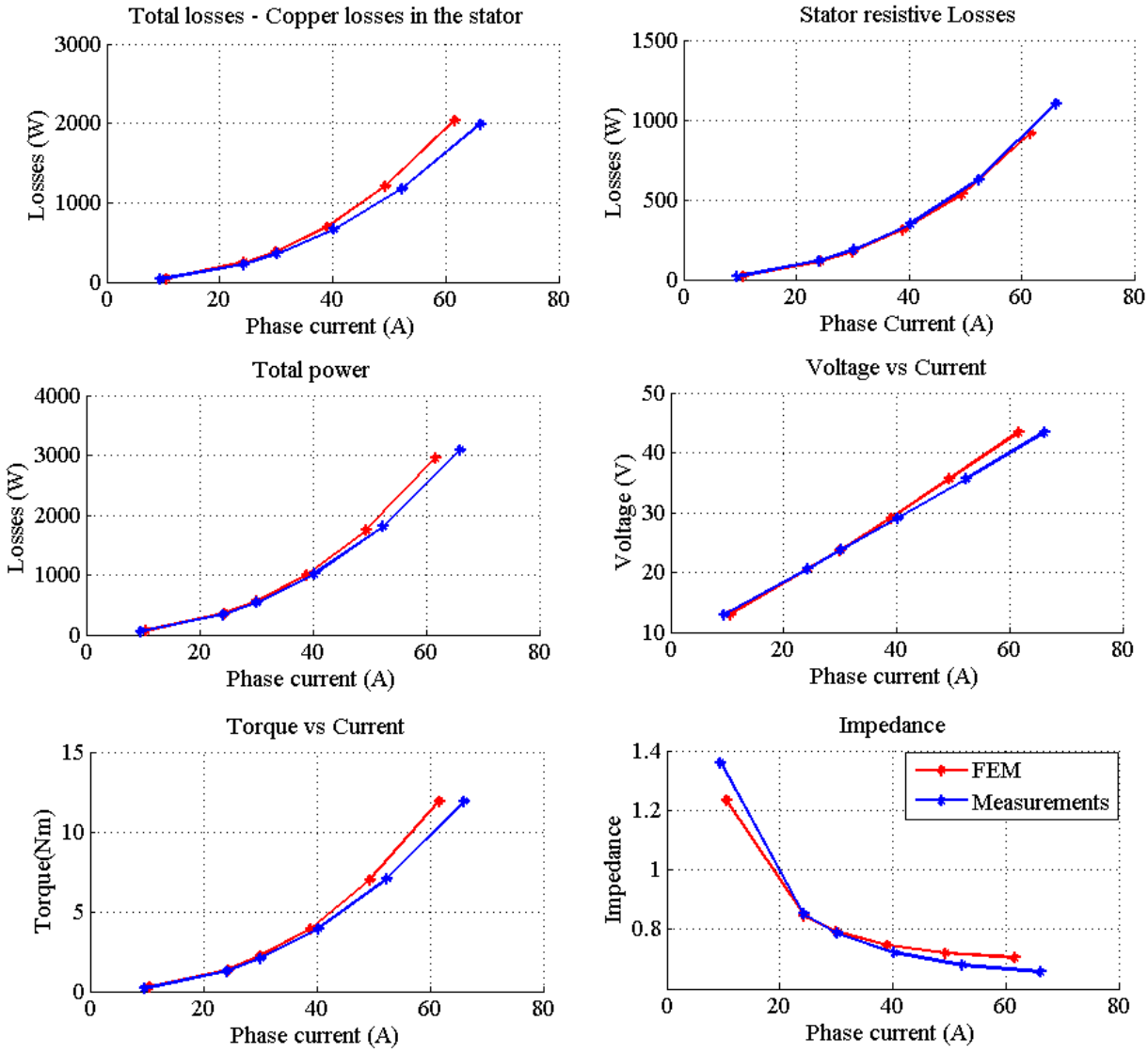

Figure 3.9: Comparison of measurements and FEM for a non-skewed machine

The measurement agrees with the simulation and thus validated. We already have validation model for a non-skewed machine. In-order to validate the skewed measurements a Magnetic equivalent circuit was used.

4 Magnetic equivalent circuit model (MEC)

Skewing was modelled by the author of the paper [13] by using a simple magnetic equivalent circuit model. This could be a tool from which the measurements could be validated, or else the model could be validated.

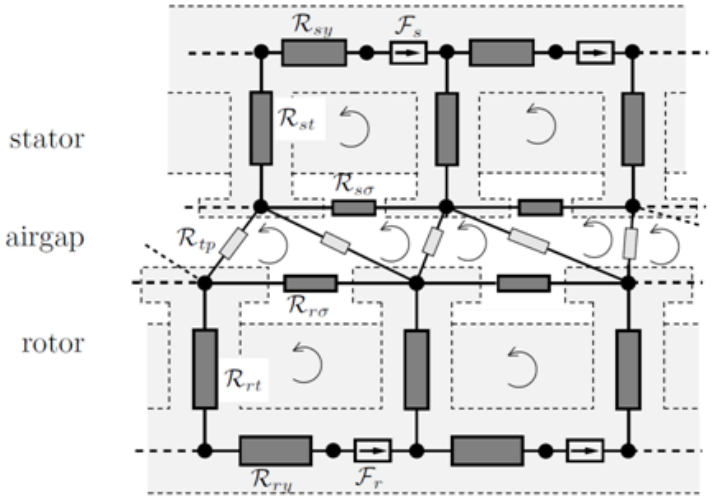

Figure 4.1: Formulation of the MEC model;[13]

As show in Fig 4.1, the magnetic equivalent circuit was build up by the author assuming that the whole magnetic circuit is built up of basic reluctance elements comprising of the yoke, tooth and the reluctance due to the leakage reactance. These reluctances are characterized as rectangular elements derived using the following formula.

$$Rel = \frac{len}{\mu A} \tag{4.1}$$

Where,

Rel:	Reluctance of the element
len:	Length of the reluctance element along which the flux flows
A:	Area of the cross section along which the flux flows
μ:	Permeability of the reluctance element.

In addition to this, the reluctance in the air-gap is modelled by an analytical function show by the Fig 4.2 which depends on four parameters $[d1, d2, d3, d4]$. These parameters are fitted before using it in the MEC model by using a FEM model.The source of mmf driving the fluxes are the stator mmf through the stator windings and the rotor mmf driven by the rotor bar currents. Flux loops as shown in Fig 4.3 were depicted using matrices, and flux through each element of the system could be calculated. The author models the effect of skewing and the inter-bar currents by means of a multi-slice model similar to a mutli-slice FEM. This is illustrated in

Fig 4.3. The slices can be distributed either uniformly or using the Gauss scheme along the length of the machine. The author illustrates that using a Gauss scheme gives an added advantage on the speed of the calculation. This multi-slice analytical model also takes into account the effect of inter-bar resistance in the rotor cage as lumped parameter between the bars. The value of inter-bar resistance could be measured from the rotor and is fed to the model. A suitable method to measure the inter-bar resistance should also be determined. The details about the type of inter-bar resistance measurements and its measurement set-up is discussed in detail in the coming sections.

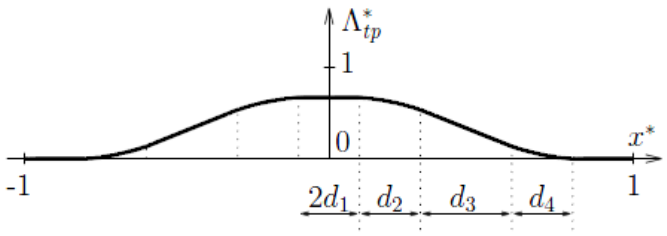

Figure 4.2: Analytical function for defining the air gap reluctance;[13]

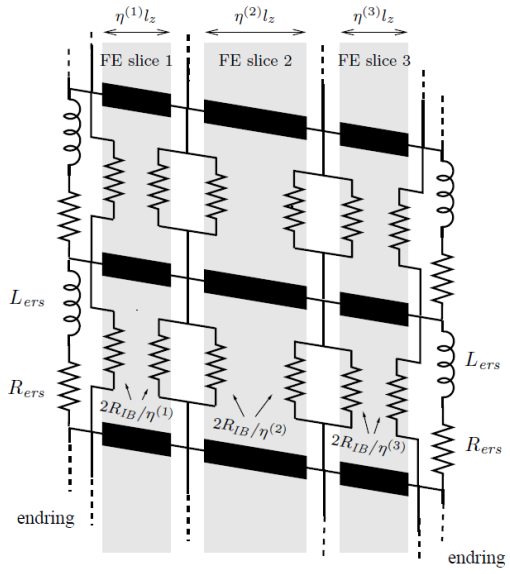

Figure 4.3: Multi slice electrical circuit model;[13]

In the above figure η represents a dimensionless coefficient, which defines how the slices are discretized along the length of the shaft. For a normal distribution of slices in the rotor, the slices would be of equal sizes.

$$\eta = \frac{1}{n_s} \tag{4.2}$$

where n_s is the number of slices.

Also both the effect of endwindings and the endrings are considered by using the lumped parameters R_{ers} and L_{ers} in the equivalent circuit.

4.1 Validation of the MEC model

After the parameters in the MEC model were adjusted to the 37 kW induction machine, the model needs to be validated using FEM. Using the already available template in fcsmek for the induction machine, magnetostatic calculations were carried out for different stator currents. The flux linkage in both the model were compared and analysed.

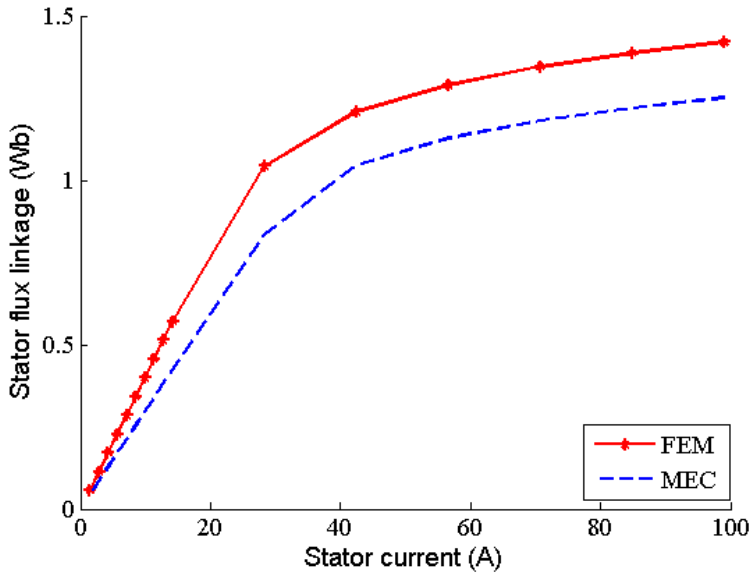

Figure 4.4: Comparison of MEC model and static FEM with closed rotor slots

The results from FEM and MEC didn't seem to match (Fig 4.4). The MEC model was modelled for an open rotor slot machine by the author. So, the geometry in fcsmek was changed to a open rotor slot design maintaining the dimensions of the teeth and the slot.

The parameters for the real machine was changed and these value were also changed in both fcsmek and the MEC model. The parameters are listed in the Table 4.4 and the new rotor slot geometry is given in the Fig 4.5.

Table 4.1: Rotor slot parameters

Parameters	Values(mm)
H21	0.70
H23	32.50
B21	2.00
B22	6.00
B11	3.50

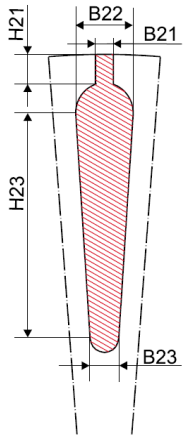

Figure 4.5: Open rotor slot;[14]

As mentioned before, the air-gap reluctance is defined by an analytical function with four variables [d1, d2, d3, d4]. These four variables were fitted to a finite element model by the author so that the model predicts the correct value. Similar type of fitting is also done in our model, so that the ouput from fcsmek matches the output from the MEC model. The constraint optimization was done using genetic algorithm in MATLAB. This optimization runs till both the results matches in FEM and MEC.

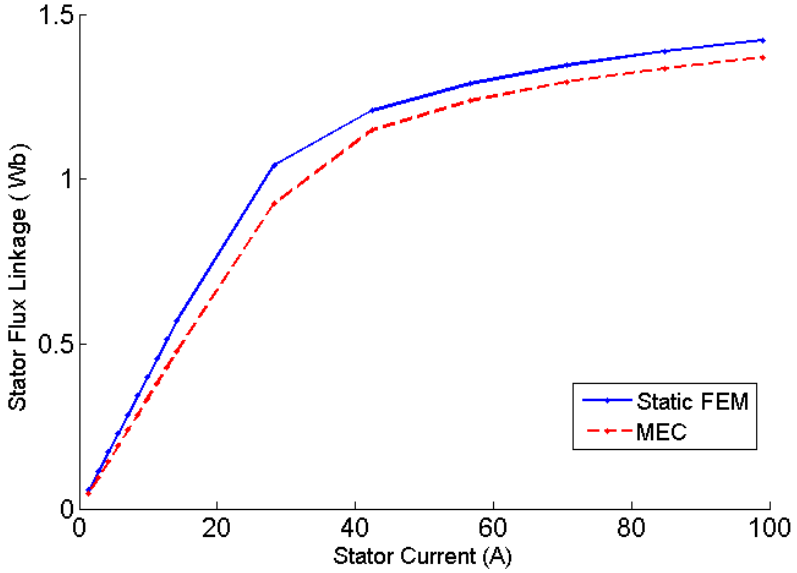

Figure 4.6: Fitting the airgap parameters between MEC and FEM by changing the air gap parameters

Figure 4.6 gives the output for the fitting between the MEC and FEM. On analysis of the output there was a change of almost 5% between both the curve. The problem was assumed to be that the effect of stacking of iron laminations were not considered in the MEC model. So the fitting was done again neglecting the effect of stacking in the steel laminations.

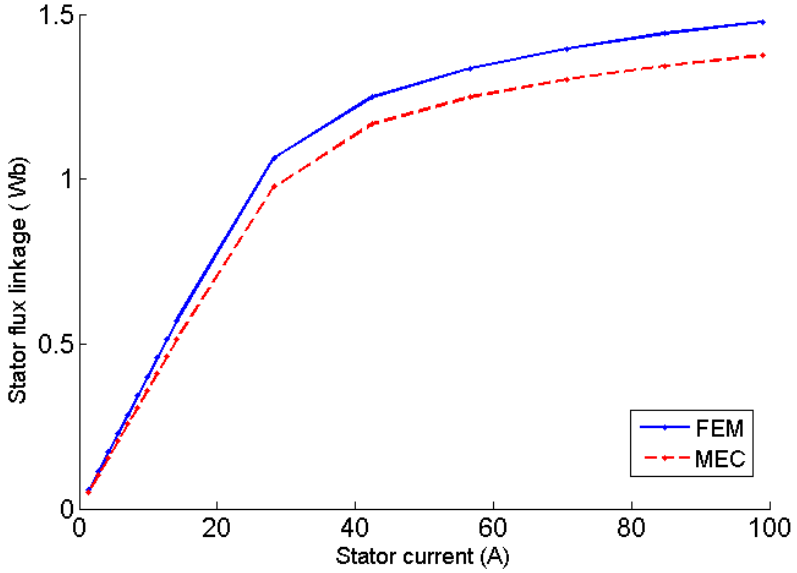

Figure 4.7: Fitting the air-gap parameters between MEC and FEM by changing the air gap parameters and neglecting the effect of stacking

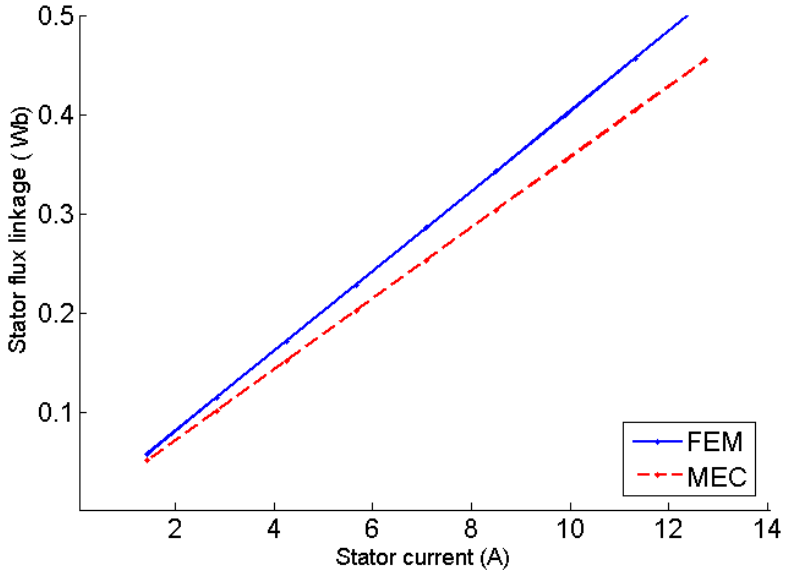

Figure 4.8: Fitting the airgap parameters between MEC and FEM by changing the air gap parameters in the linear region

The linear region in the machine was found to be close with FEM results (Fig 4.7) during the second fitting, but as the machine reached saturation the error between the two curves were becoming larger. To narrow down the problem, the machine

was simulated only in the linear region with lesser number of points and checked if the curves would fit.

Even with lesser number of points and simulating the machine only in the linear region, the fitting of the air gap parameters doesn't seem to make the curve match (Fig 4.8). The definition of all the reluctance elements in the MEC model for the stator and rotor slots is somewhat different from what had been assumed in FEM. The next step would be to use a simpler geometry for rectangular slots in both the stator and rotor.

4.2 Comparison of MEC model and static FEM with rectangular slots

Keeping the original dimensions intact the shape of both stator and rotor slots were changed as given in the tables 4.2 and 4.3. The new rectangular shape of the slots are given in the Fig 4.9.

- Rectangular stator slot dimensions

Table 4.2: Stator slot parameters

Parameters	Values (mm)
H1	23.90
H13	20.50
B11	6.54

- Rectangular rotor slot dimensions

Table 4.3: Rotor slot parameters

Parameters	Values (mm)
H2	33.50
B21	5.50
B22	15.50

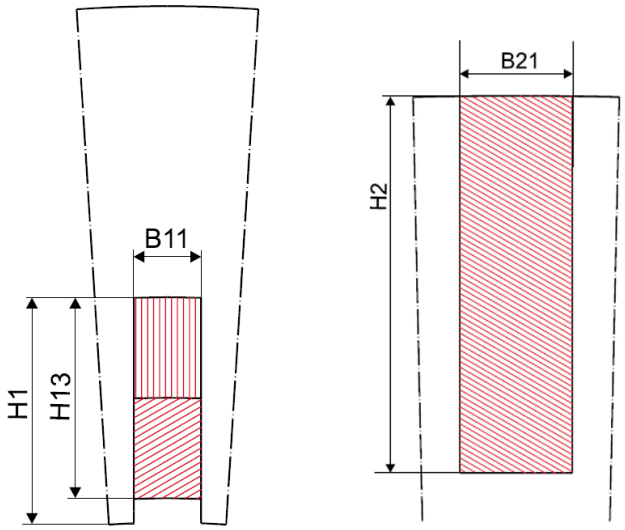

Figure 4.9: Rectangular stator and rotor slots;[14]

After changing the slots shapes in FEM model, similar fitting with the air-gap parameters was again done for a linear machine.

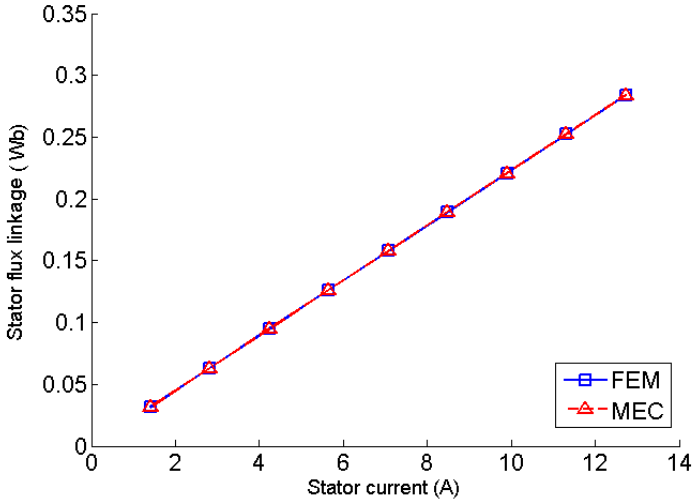

Figure 4.10: Fitting the air-gap parameters between MEC and FEM by changing the air gap parameters for a linear machine with rectangular slots

The fitting results (Fig 4.10) from the above analysis is matching pretty well with each other. We can infer from this output that the MEC model is made up of simple reluctance network with rectangular shape and lesser number of elements, to improve speed of computation. The next step would be to compare the fitting results with the effect of saturation.

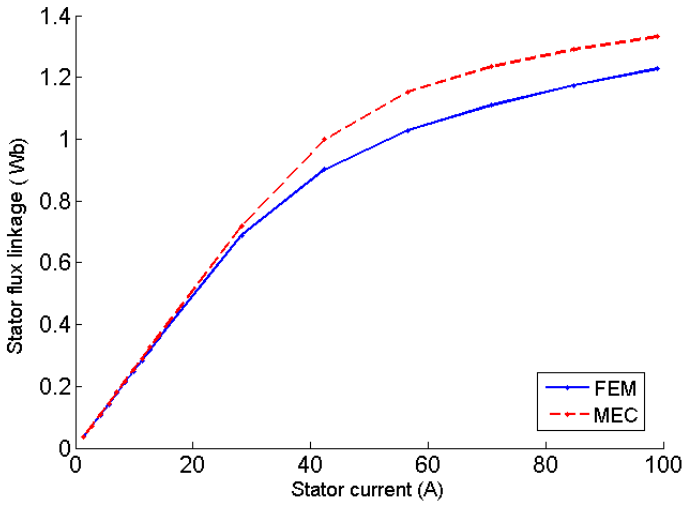

Figure 4.11: Fitting the air-gap parameters between MEC and FEM by changing the air gap parameters with rectangular slots and including the effect of saturation

The output (Fig 4.11) is fitting well in the linear region, but still there is some error in the non linear region. To analyse the problem more deeply, both the stator and rotor can be analysed part by part.

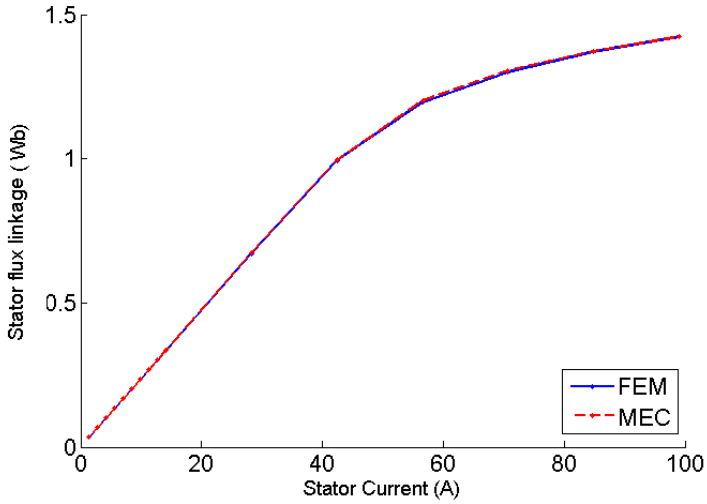

Figure 4.12: Fitting the air gap parameters between MEC and FEM by optimizing the width of the stator slots and keeping the rotor linear for a machine with rectangular slots

The first step is to change only the material property of the rotor to a linear material in FEM and then a similar fitting is done. But this time both the air gap parameters and width of the stator slots are optimized in the MEC model. The sum

of the length of tooth and the width of the yoke are put as a constant, which is a constraint to the optimization algorithm.

These fitting results have resulted to be the most promising and also justify our assumptions. The plot (Fig 4.12) shows that both FEM and MEC yield to a same result. Now the material for the stator is kept linear and both rotor slot dimensions as well as the air gap parameters are set as variables for the optimization algorithm.

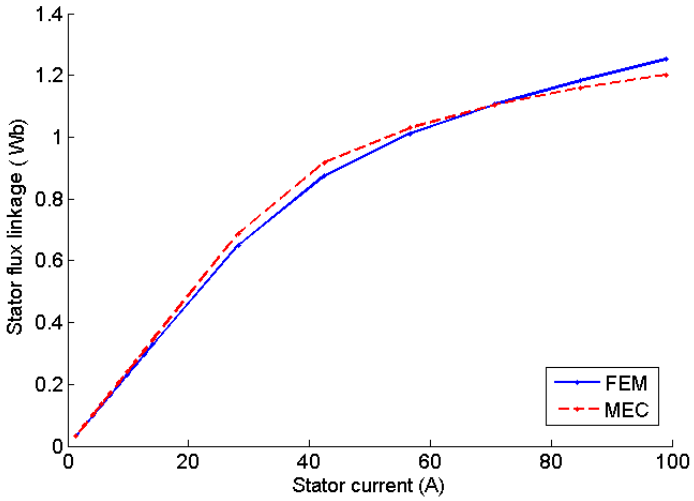

Figure 4.13: Fitting the air gap parameters between MEC and FEM by optimizing the width of the rotor slots and keeping the stator linear for a machine with rectangular slots

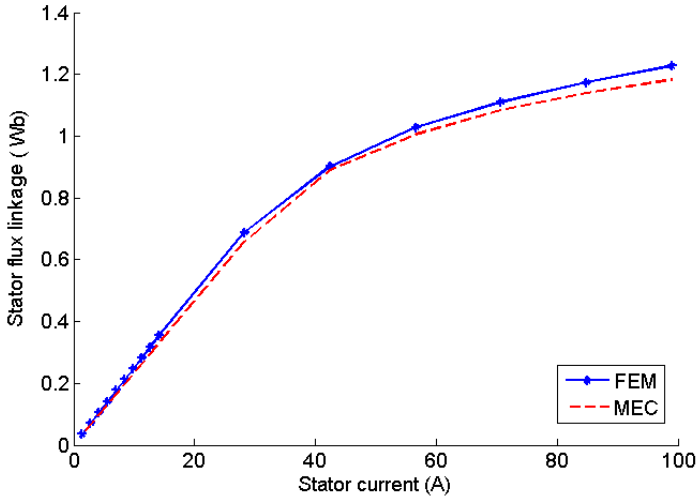

Figure 4.14: Comparison of MEC and FEM output with the parameters obtained from optimization for the machine with rectangular slots

The fitting results of the MEC model with FEM are found to be satisfactory, but with small differences (Fig 4.12). The resulting dimensions from the above 2 analysis are fed to the MEC model and now FEM and MEC model results are compared.

Now we have validated the MEC model for a 37 kW machine with rectangular slots (Fig 4.14). The next step would be to extend this analysis method onto the machine, but now with the original slot shapes and open rotor slots. As done before, at first the rotor is kept linear and the dimensions of stator slots are optimized (Fig 4.15).

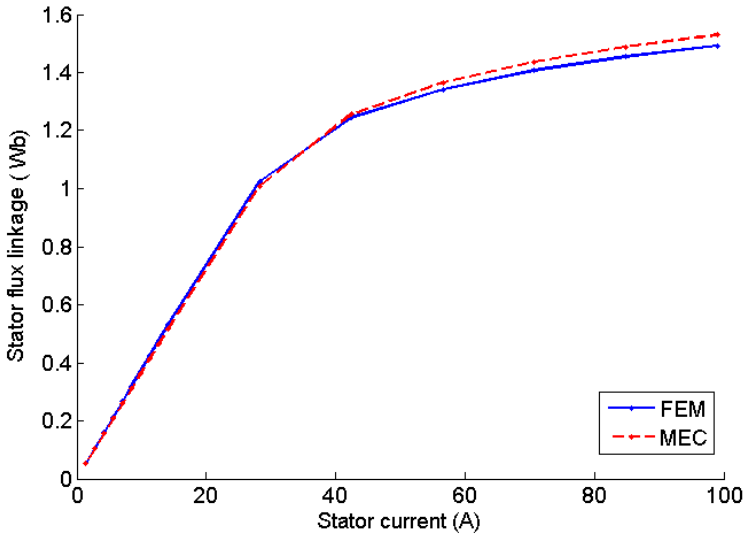

Figure 4.15: Output after fitting MEC and FEM by optimization of stator dimensions keeping the rotor linear with original slot shapes and open rotor slots

Now the stator is kept linear and the dimensions of the rotor are optimized to fit both the plots.

While the MEC model easily fitted to the FEM results, when the rotor was kept linear and had rectangular slots, in the second case where the stator is linear, the results didn't seem to fit with the FEM results (Fig 4.15).

Fitting was done again by optimizing both the stator and rotor slot dimensions simultaneously. This is as close the MEC model fits with the FEM model and the dimensions were noted down for feeding to the MEC model (Fig 4.14).

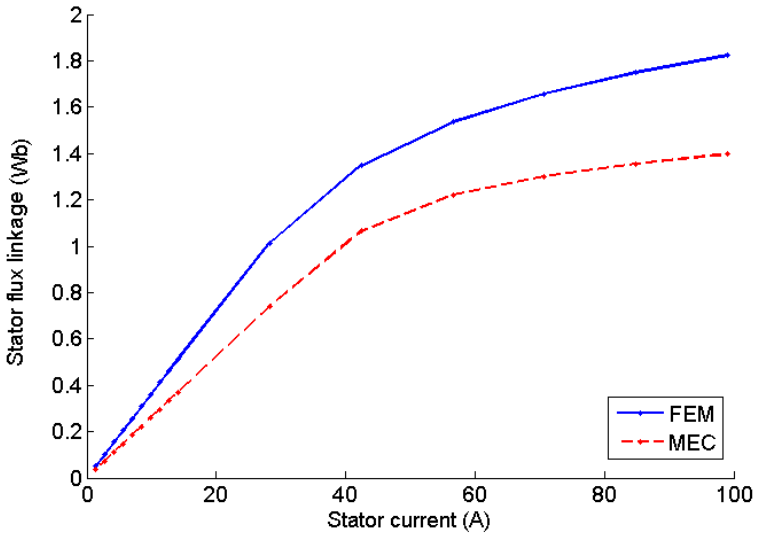

Figure 4.16: Output after fitting MEC and FEM by optimization of rotor dimensions keeping the stator linear with original slot shapes and open rotor slots

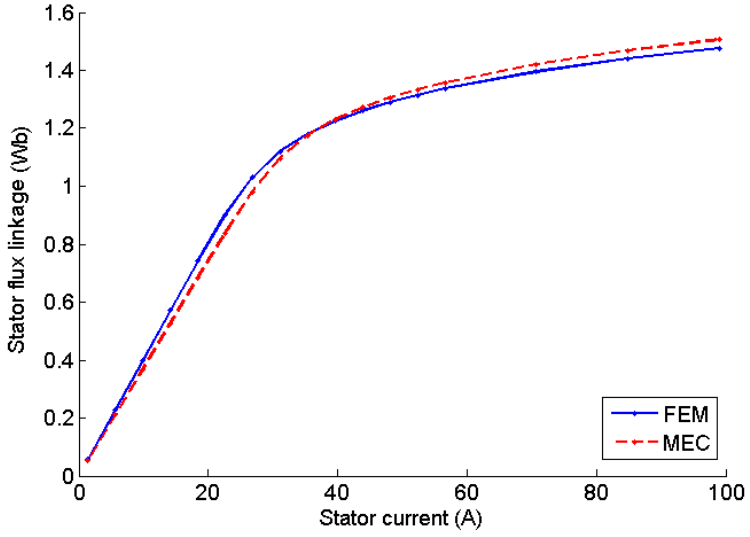

Figure 4.17: Output after fitting MEC and FEM by optimization of both stator and Rotor dimensions

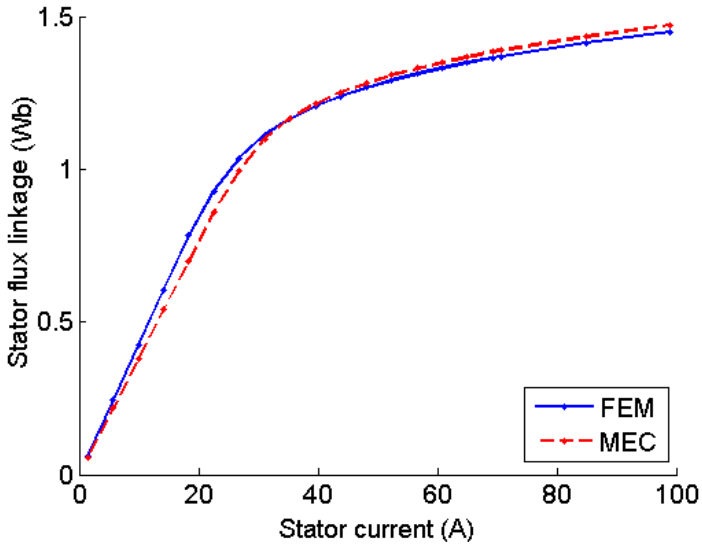

Figure 4.18: Output after fitting MEC and FEM by optimization of both stator and rotor dimensions for a closed rotor

The fitting was done again now for a closed rotor machine by optimizing the width of both stator and rotor slots and the results are show in Fig 4.17.

Now with the fitting results and parameters from the above analysis, we have a model which gives you the same output as that of a non-skewed FEM model. This could be used to compare the measurements and validate them. On the other hand the accuracy of the model with the original parameters could be increased by increasing the number of reluctance elements in the model and also by changing the reluctance shape to more realistic shapes as shown below (Fig 4.18).

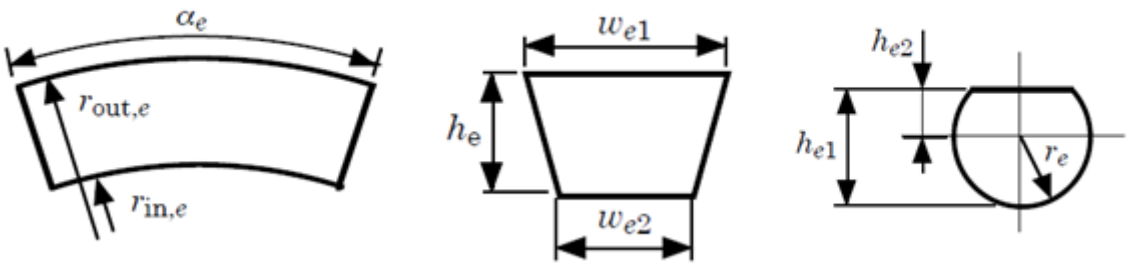

Figure 4.19: Reluctance elements;[15]

5 Inter-bar resistance measurement setup

Another experiment which can be conducted in this work would be to estimate the inter-bar resistance of the skewed as well as the non-skewed rotor. There are many ways by which the inter-bar resistance of an induction machine can be measured. Some of these methods have been discussed in the paper [7]. Of these methods some require destruction of the rotor while others don't. A non-destructive measurement setup was constructed by Stening in his work [8]. A similar setup was made in this analysis to support the existence of inter-bar currents.

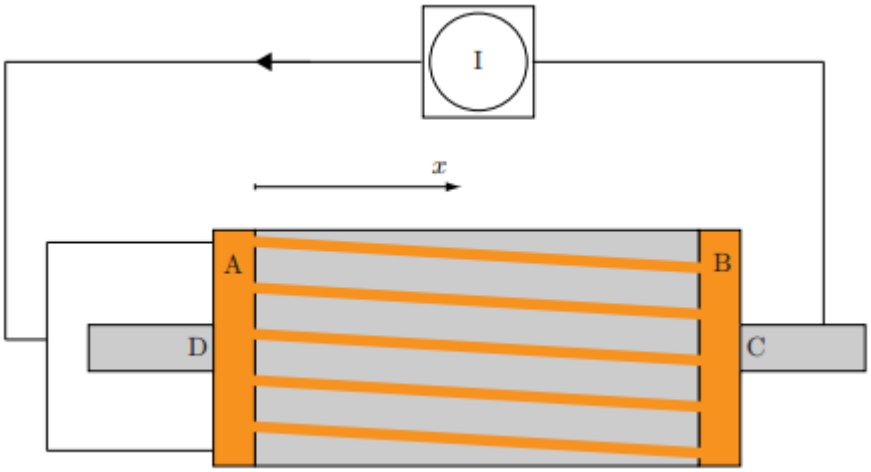

Figure 5.1: Inter-bar resistance measurement;[8]

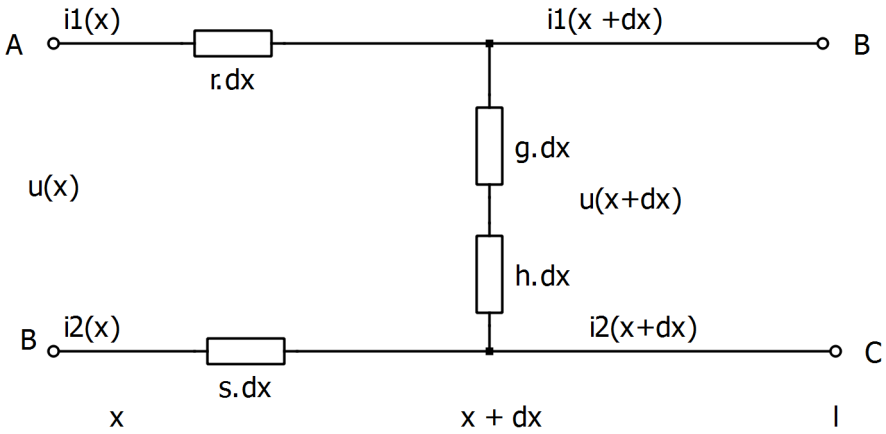

Figure 5.2: Equivalent circuit representation of the rotor

In Fig 5.2, the rotor is represented by means of a simple equivalent circuit, here r - bar resistivity per unit length ; s - shaft resistivity per unit length ; g - contact

conductivity per unit length ; h - electrotechnical iron sheet conductivity per unit length ;l - rotor length and dx is the elementary section of the rotor axially. Based on this equivalent circuit shown in the figure, the following differential equations could be derived and solved by applying the boundary conditions, obtained by measurements of U_{ad} ,U_{bc} and U_{ab}. These are the voltage measured across the points A,B,C,D on the rotor of the machine as shown in Fig 5.1.

$$\begin{cases} \dfrac{du(x)}{dx} = si_2(x) - ri_1(x) \\ \dfrac{di_1(x)}{dx} = -\dfrac{gh}{h+g}u(x) \\ \dfrac{di_2(x)}{dx} = \dfrac{gh}{h+g}u(x) \end{cases} \tag{5.3}$$

Figure 5.3 shows the basic measurement set-up, A high DC current source of 600 A is required to measure the inter bar resistance. Two DC generators with ratings of 10V 300A driven by an induction motor was used as the DC current source.The DC current source was given across the shaft and the end rings of the squirrel cage rotor. In the work referenced in [8] a metal washer was used close to the end-rings to make the current-flow uniform through the bars. In order to serve the same purpose in this experiment holes were drilled in alternative fins of the end rings and cables where connected which went to a common bus bar and then to the dc generators. Shunt resistors where used to measure the current flowing through the rotor and Fluke multi-meters with crocodile clips were clipped onto the shaft and the end ring for measuring voltage.

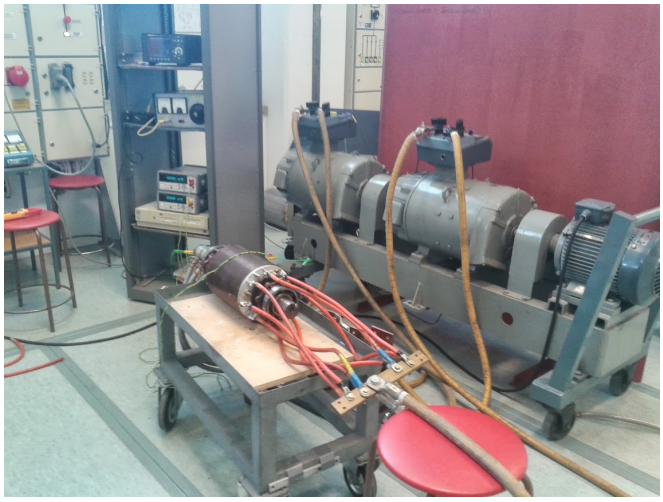

Figure 5.3: Inter-bar resistance measurement

R_q: Skewed rotor : 2.0025e-5 Ω
R_q: Non-skewed rotor : -1.5998e-5 Ω
Where Rq represents the inter-bar resistance between the rotor bars.

The values reported were obtained by solving the Eqn. 5.3. This gives a very low value of resistance between the bars in case of a skewed machine. This supports the fact that there would be currents between the bars and it would promote losses in the machine. On the other hand the measurements from the non-skewed machine gave a negative value of inter-bar resistance, which is not a feasible value.

6 More comprehensive measurements

The time stepping code for the MEC code wasn't ready, waiting for which could elongate the period of the thesis. Decision was taken that more comprehensive measurements could be taken, so that the effect of skewing could be studied further. Some measurements were done by varying the source frequency starting from 20 Hz to 50 Hz. During the measurements at lower frequencies there were reasonable vibrations in the rotor making the results of these measurements unusable. These readings have been put in the appendix section for reference. Another approach to conduct measurements would be to supply equal flux in the air-gap for both the skewed and non-skewed rotor.

6.1 Measurements with operating points as flux

The locked rotor measurements were continued with operating points as flux. For this purpose search coils were installed in each pole of the stator of the machine. As explained before, they are single turn windings which run across each pole of the winding, In this case the winding runs from the 1st slot to the 13th slot. Measurements were taken with six different operating points taking care that the flux provided in the skewed and non-skewed machine are the same.

Since the MEC model which was meant to be compared with the skewed measurements was not available, another skewed model for an induction machine was taken from the paper [16]. This model was developed at the Laboratory of Electromechanics at Helsinki University of Technology. This model was developed with reference to the same 37 kW induction machine, which was used for analysis in the thesis. The author has used a multi-slice finite element model to calculate the output from the machine to consider the effect of skewing. The author says that as the number of slices grow, so do the computation time and the accuracy. To get a compromise between the processing time and the accuracy of the model, the number of slices for the FEM was chosen as 5. The comparison of the results for the simulated models and the measurements were done and are presented below.

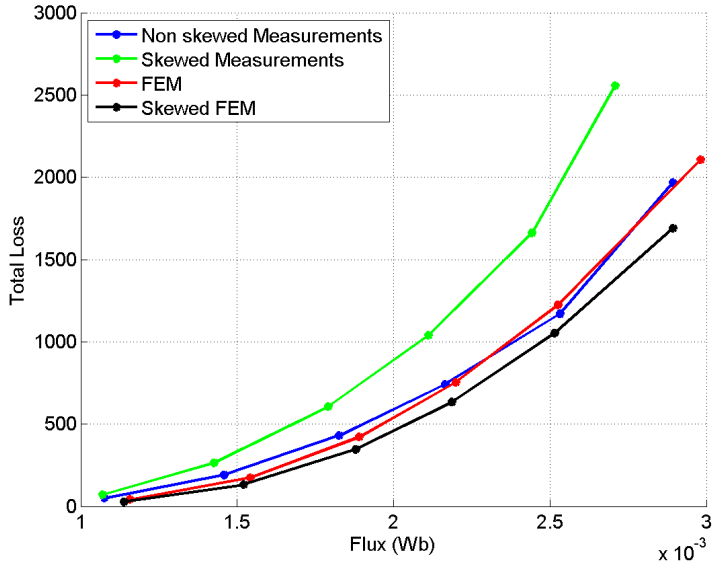

Figure 6.1: Total loss in the machine

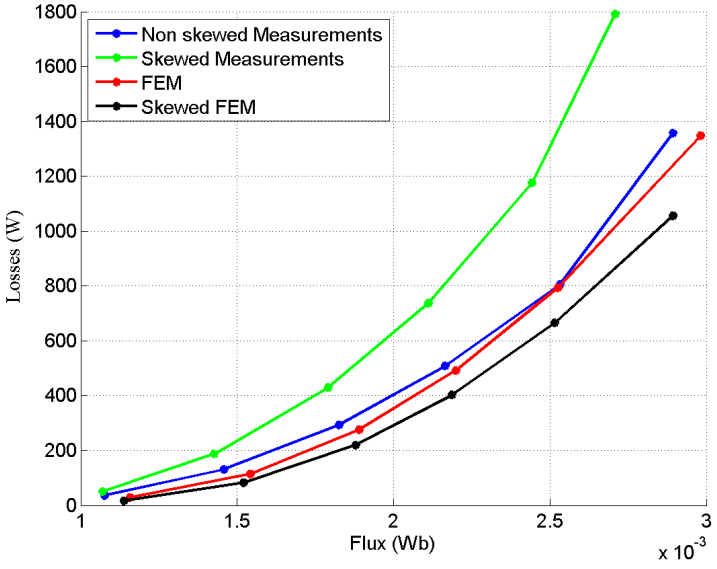

Figure 6.2: Total losses - Stator resistive losses

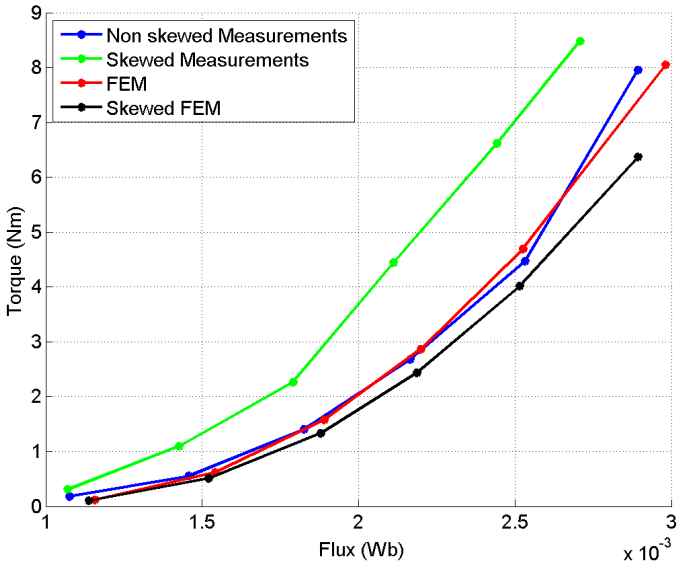

Figure 6.3: Torque

The losses in Figure 6.2 is calculated by subtracting the stator resistive losses from the total losses in the machine as mentioned in section 3.4. It can be seen from Figure 6.1 and 6.2 that there is observable difference in the losses for a skewed and a non-skewed rotor. For the same amount of flux supplied, the skewed rotor produces more amount of losses and at the same time more torque (Fig 6.3). The simulations follow nicely with the measurements for the case of the non-skewed rotor, where as the multi slice model in the paper [16] was found to be going away from the skewed measurement results. This deviation in the multi slice model can be attributed due to the absence of the consideration of inter-bar currents in the multi slice model.

6.2 Measurements with operating points as frequency

Measurements were also taken at different frequencies at constant flux to observe how the losses are affected. Some measurements where already done at different frequencies before but with frequency less than 50 Hz. These points had evident vibrations on the blocked metal bar and hence the data obtained were not usable. The results for these measurements have been kept in the appendix section. So the frequency was varied from 50 Hz to 450 Hz. Since the flux is proportional to the ration of voltage and frequency (v/f), as the frequency increases the voltage fed to the stator was also increased so that the flux remained constant at all the operating points. At higher frequencies the eddy current losses and hysteresis losses increases with frequency, and hence higher heat dissipation in the rotor. This leads to high temperature rise, especially in the rotor cage. So the measurement is started at 450 Hz and a suitable value of flux so that, the temperature of the rotor does not go higher than 200 degrees, which is the thermal limit of the rotor. This value of flux was kept constant in rest of the operating points below 450 Hz.

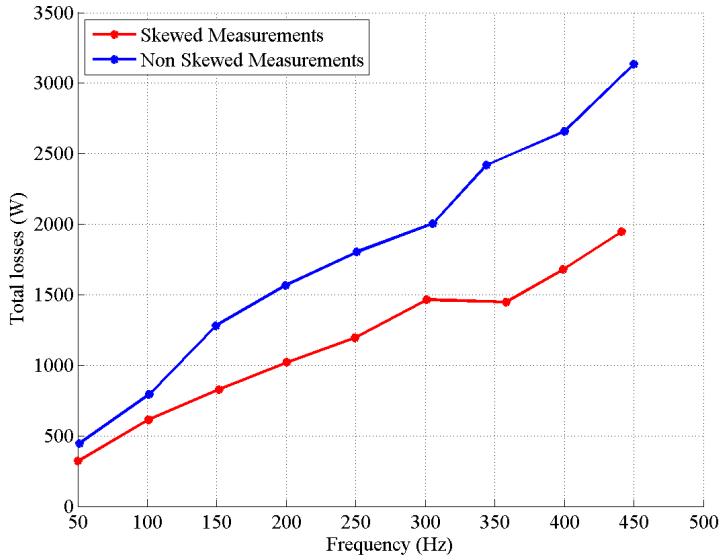

Figure 6.4: Total loss in the machine

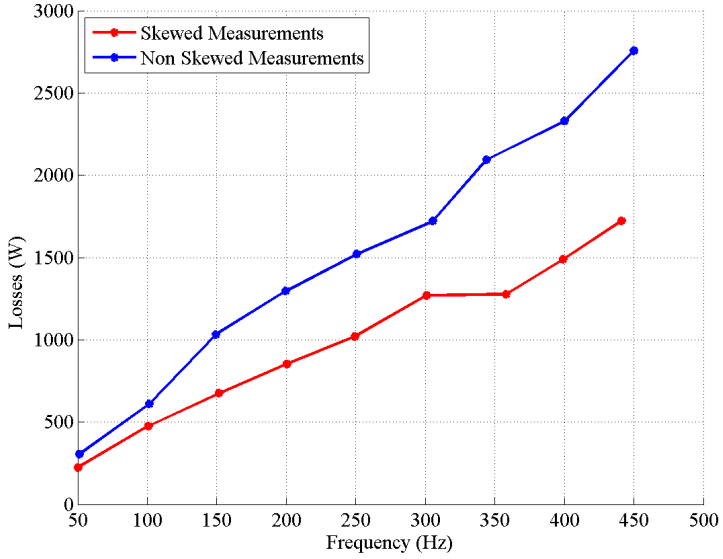

Figure 6.5: Total losses - Stator resistive losses

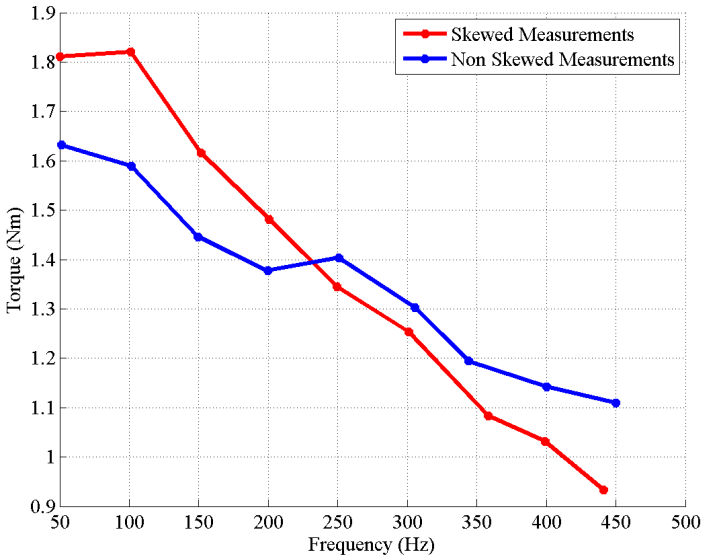

Figure 6.6: Torque

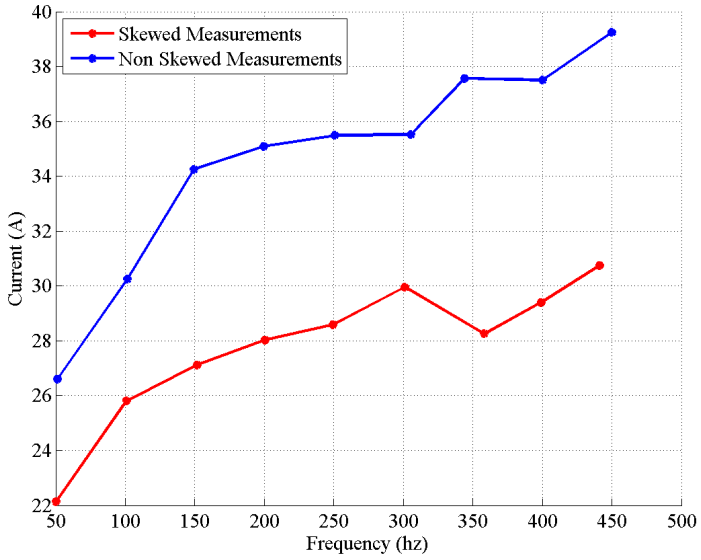

Figure 6.7: Phase current

As seen from Fig 6.4 and Fig 6.5 the losses in the non-skewed machine observed to be much more than in the skewed machine. One could also observe that the phase current in the skewed machine is much lower than the non-skewed machine. This comparison contradicts this behaviour of the skewed machine with respect to the non-skewed one.

7 Discussion and outcome

7.1 Summary

The effect of skewing in induction machine was studied with lot of measurements in different conditions. Measurement set-up was made for a locked rotor test by blocking the shaft with an iron rod. Parameters like torque, voltage, power, current and the flux induced in the air-gap were measured during this work. Each measurement was done till the machine reached thermal equilibrium as per the standards. The measurements were done keeping one of these parameters constant and compared. Finite element analysis was done using FCSMEK, and was used to validate the measurements with the non-skewed machine.

The MEC model was analyzed and was validated for the target induction machine. Parameters such as the air-gap parameters, slot dimensions of both the stator and rotor were varied in the MEC model so that the results from FEM match with MEC. Unfortunately due to the unavailability of the time stepping model of MEC, more comprehensive measurements were taken so that the effect would be elaborated. The MEC model needed the inter-bar resistance also as a parameter for the modelling of skew. Even though this model was not used, a measurement set-up was made for the inter-bar resistance measurement. While the skewed rotor gives acceptable value of inter-bar resistance, the non-skewed machine gives out a non-feasible value of resistance from the measurement.

7.2 Discussion

Keeping in mind the behaviour of losses as predicted by Williamson and McClay in the paper [10], we can start analysing and try to justify the measurement results in this work. The author says that skewing seems to alter the balance of losses between high frequency surface losses on the rotor and the iron losses on the rotor of the machine. Being a die cast rotor, the effect of inter-bar resistance could also affect these losses significantly. Being said this initial measurements in Section 3.4 with operating point as current has a higher loss for a skewed machine than the non-skewed machine. The torque also produced in this experiment was also found to be less compared to the skewed machine. This higher value of the losses could be due to the effect of inter-bar currents and the increased rotor losses in the machine.

Now going to the measurements done in Section 5.1 where measurements were done with the changing operating parameter as flux. With the same amount of flux maintained in the air-gap for both the skewed and the non-skewed machine, the losses produced in the skewed rotor are found to be higher. Supporting the reason for these increased losses in the skewed machine can be due to the inter-bar currents losses. Also the results from the multi-slice FEM model give a lesser value of losses in the skewed machine than for a non-skewed machine. This can be attributed to the absence of inter-bar current model inside the multi-slice FEM. So the increased losses in the skewed induction machine can be justified with inter-bar current losses.

Finally the measurements in Section 5.2 with different frequencies as operating

point have a flipped behaviour of losses as from the previous measurements. As the frequency increased, the losses in a non-skewed machine were found to be much higher than the skewed machine. This means that the extra high frequency joule losses or the surface losses on the rotor are higher than the combined losses due to the inter-bar currents and the increased iron losses in the machine due to skewing.

7.3 Conclusion

A rather preliminary investigation on the effect of skewing was done in this thesis for a 37 kW induction machine. With measurements, it was found that skew aids the flow of inter-bar current losses in the machine and hence increases the joule losses in the machine. Measurements at higher frequencies showed that the rotor joule losses are significantly reduced in the rotor cage of a skewed induction machine compared to a non-skewed induction machine. These measurements have shown that skewing has a significant effect on the harmonics produced in the air-gap. Therefore the decision to skew a machine depends more on the application where the motor would be used and all motor parameters. All these measurements were done with the rotor stationary, more load tests with a rotating rotor can be done and the torque-speed curves could be compared for a skewed and a non-skewed machine in future works.

8 References

[1] Belahcen, A. (2012) *S-17.2030, Electromechanics and Electric Drives, Lecture notes* at Aalto University, Espoo, Finland.

[2] Nishizawa, H., Itomi, K., Hibino S. and Ishibashi F. (1987) *Study on reliable reduction of stray losses in three-phase induction motor for mass production.* In: *IEEE Transactions on Energy Conversion, Vol. EC-2,No. 3, September 1987.*

[3] Kirtley J. (n.d) *Machinery, Chapter 15, Massachusetts Institute of Technology* Available from: http://www.rle.mit.edu/media/pr152/15_PR152.pdf [Accessed on 29 January 2014]

[4] Pyrhönen, J., Jokinen, T.& Hrabovcovà, V. (2008), *Design of rotating electrical machines*, Wiltshire: John Wiley & Sons, Ltd.

[5] Englebretson, S. C. (2009) *Induction Machine Stray Loss from Inter-bar Currents.* PhD Thesis. Cambridge, USA: Massachusetts Institute of Technology [published].

[6] Odok, A.M. (1958) *Stray-Load Losses and Stray Torques in Induction Machines.* In:*Power apparatus and systems, part iii. transactions of the american institute of electrical engineers (Volume:77, Issue: 3), Page(s) 43 - 53.*

[7] Dabala., K. (2006) *Modified method to determine rotor bar-iron resistance in three phase copper casted squirrel-cage induction motors.* In: *Proceedings of the 17th International Conference on Electrical Machines, Chania, Crete Island, Greece, 2-5 September 2006.*

[8] Stening, A. (2013) *Analysis and Reduction of Parasitic Effects in Induction Motors With Die-Cast Rotors.* PhD Thesis. Stockholm, Sweden: KTH [published].

[9] Williamson, S. and Smith, A.C. (2002) *Influence of Inter-bar currents on the harmonics losses and skew in cage induction machines* In: *Power Electronics, Machines and Drives, 2002. International Conference on (Conf. Publ. No. 487), 4-7 June 2002.*

[10] McClay, C.I. and Williamson, S. (1998) *The Variation of Cage Motor Losses with Skew.* In: *Industry Applications Conference, 1998, St. Louis, MO, USA, 12 Oct 1998-15 Oct 1998*

[11] Geuzaine, C. and Remacle J.(n.d) *Gmsh: a three-dimensional finite element mesh generator with built-in pre- and post-processing facilities* Available from: http://geuz.org/gmsh/doc/texinfo/gmsh.html#Tutorial [Accessed on 29 January 2014]

[12] Standard IEC 61972, IEEE *Method for Determining Losses and Efficiency of Three-Phase Cage Induction Motors*, 2G/102/CDV, August 1998.

[13] Gyselinck, J., Sprooten J., and Lòpez-Fernàndez, X.M. (2006) *Multi-Slice FE and MEC Modelling of Induction Motors having a Broken Bar: Influence of Inter-Bar Currents and Bar Breakage Location.* In: *Proceedings of the 17th International Conference on Electrical Machines, Chania, Crete Island, Greece, 2-5 September 2006.*

[14] Arkkio, A. and Dlala, E. (2008) *FCSMEK, PART D, USER'S GUIDE*, Helsinki University of Technology.

[15] Perho, J. (2002) *Reluctance network for Analysing induction Machines.* PhD Thesis. Helsinki, Finland: Acta Polytechnica Scandinavica [published].

[16] Tenhunen, A. and Arkkio, A. (2001) *Modelling of induction machines with skewed rotor slots* In: *IEE Proceedings - Electric Power Applications, Vol. 148, No. 1, January 2001, pages 45-50.*

Appendix- A

The Machine Parameters

The MEC model used in this thesis needs parameters for the 37 kW induction machine used for measurement. Some of the parameters of the machine are as follows:-

- Length of the machine $\mathbf{l}_{machine}$: 249 mm
- Number of Pole pairs: 4
- Number of slots per pole and phase: 4
- Number of turns in a slot: 6 (The actual number of turns in the machine was 12, but we have two parallel paths in the machine and hence 6).
- Resistance of one stator phase = 0.0645 (Measured during testing)
- Number of rotor bars = 40
- Resistance of one rotor bar = 84.412e-6 (Got from Fcsmek)
- Resistance of one end ring segment = .8142e-6
- Inductance of End ring segment= 4.914e-9
- Skew and inter-bar parameters are not considered, since we are just trying with a non skewed model first.
- There are no broken bars also.
- Axial Length of the Machine = .249 m
- Stator Parameters : -

  Length of stator teeth $\mathbf{l}_{st}$:23.9 mm
  Width of stator teeth $\mathbf{w}_{st}$:7.4 mm
  Length of stator slot $\mathbf{l}_{ss}$:23.9 mm
  Width of stator slot $\mathbf{w}_{ss}$:8.8 mm
  Length of stator yoke$\mathbf{l}_{sy}$:18.2 mm
  Width of stator yoke $\mathbf{w}_{sy}$:31.1 mm

- Rotor Parameters :

  Length of rotor teeth $\mathbf{l}_{rt}$:33.9 mm
  Width of rotor teeth $\mathbf{w}_{rt}$:9.732 mm
  Length of rotor slot $\mathbf{l}_{rs}$:33.9 mm
  Width of rotor slot $\mathbf{w}_{rs}$:5.85 mm

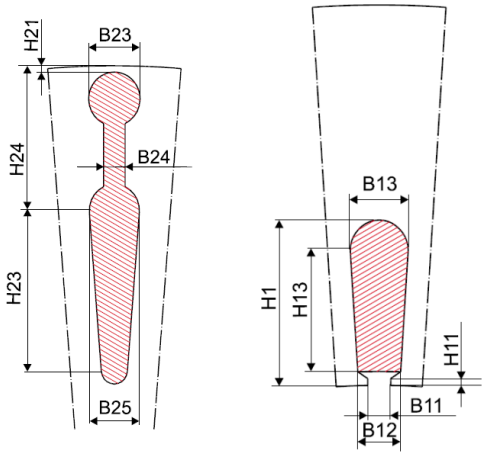

Figure 8.1: Shape of the stator and rotor slots.[From Fcsmek manual]

Table 8.1: Stator Slot Parameters

Parameters	Values(mm)
B13	8.80
H1	23.90
H13	17.50
H13	1.00
H11	1.00
B11	3.50
B11	6.50

Length of rotor yoke$\mathbf{l}_{ry}$:7.87 mm
Width of rotor yoke $\mathbf{w}_{ry}$:30.3 mm

Table 8.2: Rotor Slot Parameters

Parameters	Values(mm)
H21	0.70
H23	17.80
H24	16.10
B23	6.00
B24	2.50
B25	5.85

Appendix- B

Results with operating point as frequency

Some measurements were also taken with different frequencies for both the skewed and the non skewed rotor from 20 Hz to 50 Hz. Current was kept constant at the nominal rated load for these measurements. The data procured from these measurements are not stable and accurate. During measurements below the rated frequency of 50 Hz there were evident vibrations which have disrupted the measurements.

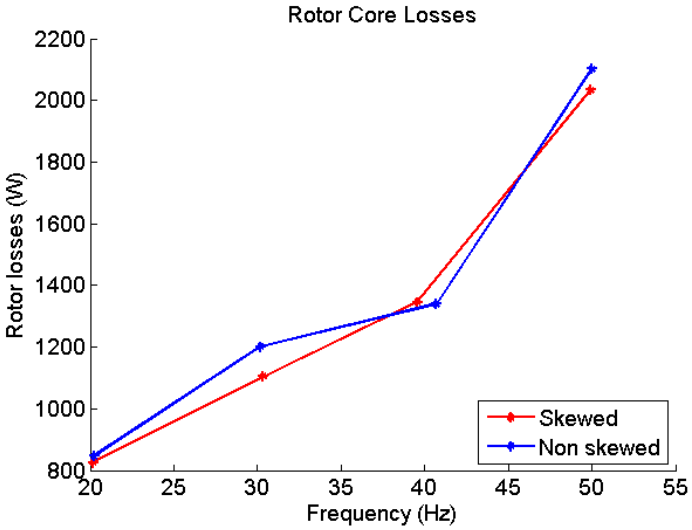

Figure 8.2: Comparison of rotor core losses in both skewed and non skewed rotor

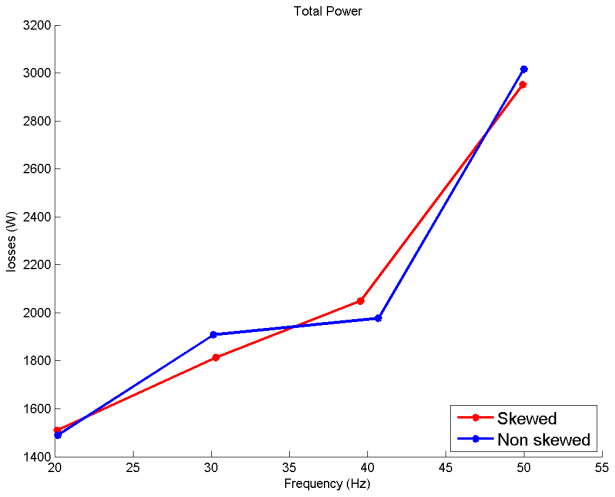

Figure 8.3: Comparison of total power losses in both skewed and non skewed rotor

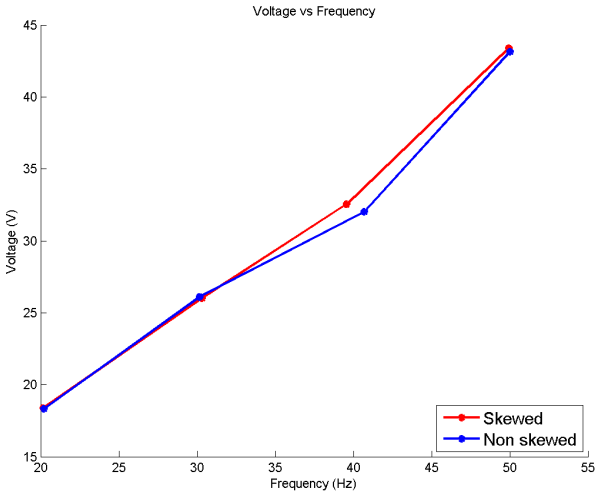

Figure 8.4: Voltage plots of both skewed and non skewed rotor

Results with operating point as torque

Using the torque measurement setup, losses were plotted against torque and the results are shown as below. These data where taken from the measurement in section 3.4 ,where the stator current was changed in both the rotors and the frequency was kept at 50 Hz.

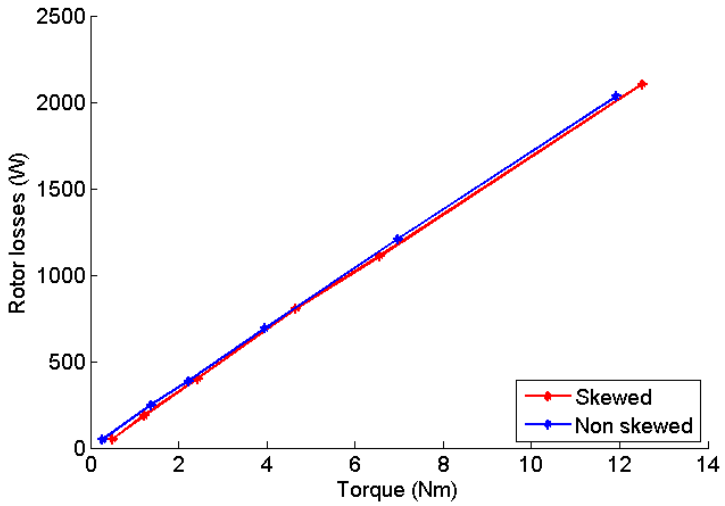

Figure 8.5: Comparison of rotor losses in both skewed and non skewed rotor

Interestingly, when the losses where plotted against torque, the losses due to the Non-skewed is greater than the skewed one by a minute amount. Also in Fig 5.11 the skewed machine requires less amount of current to produce the same amount of torque.

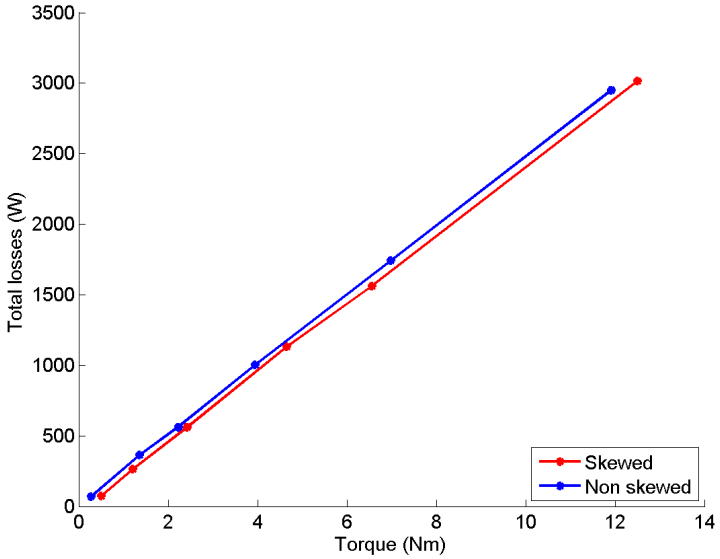

Figure 8.6: Comparison of total power losses in both skewed and non skewed rotor

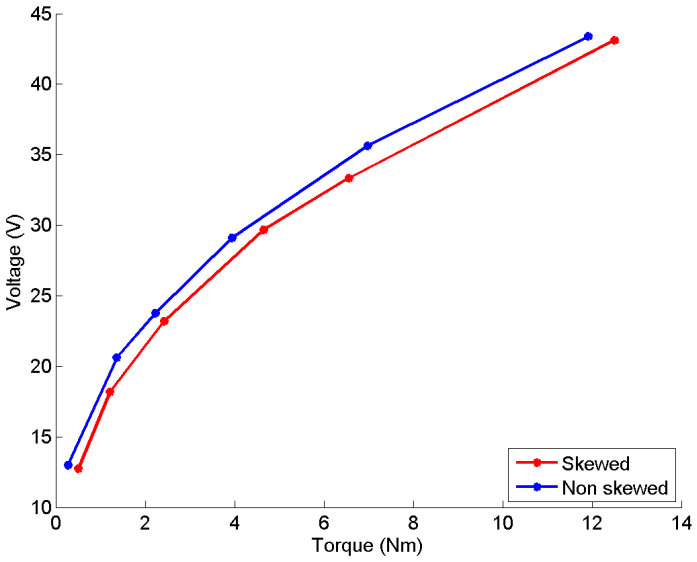

Figure 8.7: Voltage plots of both skewed and non skewed rotor

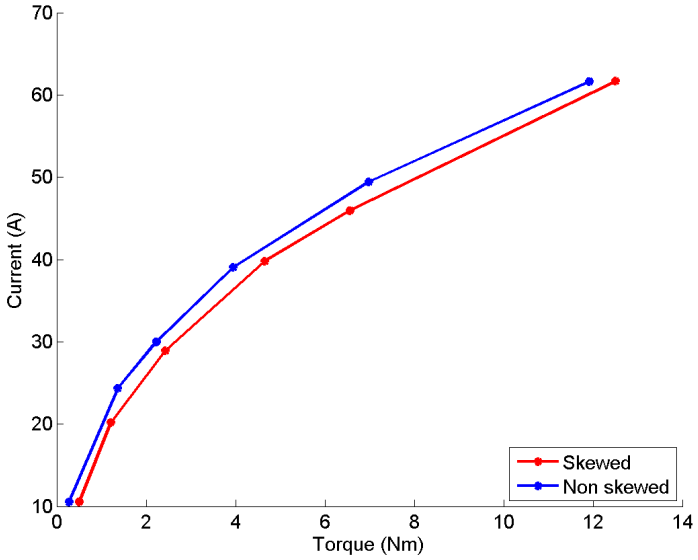

Figure 8.8: Current plots of both skewed and non skewed rotor

Appendix- C

Summary of all the values

The change in parameters in different cases of analysis have been described. In all the cases the following parameters $[d1, d2, d3, d4]$,$\mathbf{l}_{machine}$,$\mathbf{l}_{st}$,$\mathbf{w}_{sy}$,$\mathbf{l}_{rt}$, and $\mathbf{w}_{ry}$ have been obtained after analysis. The rest of the parameters are the same as described in the motor parameters section.

Table 8.3: Summary of parameters

1.Closed rotor slots					
[d1 d2 d3 d4]	$\mathbf{l}_{machine}$	$\mathbf{l}_{st}$	$\mathbf{w}_{sy}$	$\mathbf{l}_{rt}$	$\mathbf{w}_{ry}$
[0.079 0.063 0.760 0.096]	236.55	23.9	31.1	33.9	30.3
2.Open rotor slots					
[d1 d2 d3 d4]	$\mathbf{l}_{machine}$	$\mathbf{l}_{st}$	$\mathbf{w}_{sy}$	$\mathbf{l}_{rt}$	$\mathbf{w}_{ry}$
[0.079 0.063 0.760 0.096]	236.55	23.9	31.1	33.9	30.3
3.Air gap parameters from Gyselinck					
[d1 d2 d3 d4]	$\mathbf{l}_{machine}$	$\mathbf{l}_{st}$	$\mathbf{w}_{sy}$	$\mathbf{l}_{rt}$	$\mathbf{w}_{ry}$
[0 0.0481 0.231 0.287]	236.55	23.9	31.1	33.9	30.3
4.Fitting the air-gap parameters					
[d1 d2 d3 d4]	$\mathbf{l}_{machine}$	$\mathbf{l}_{st}$	$\mathbf{w}_{sy}$	$\mathbf{l}_{rt}$	$\mathbf{w}_{ry}$
[0.073 0.151 0.758 0.018]	236.55	23.9	31.1	33.9	30.3
5.Fitting the air-gap parameters by neglecting the effect of stacking					
[d1 d2 d3 d4]	$\mathbf{l}_{machine}$	$\mathbf{l}_{st}$	$\mathbf{w}_{sy}$	$\mathbf{l}_{rt}$	$\mathbf{w}_{ry}$
[0.079 0.063 0.760 0.096]	249	23.9	31.1	33.9	30.3
6.Fitting the air-gap parameters by neglecting the effect of stacking only in the linear region					
[d1 d2 d3 d4]	$\mathbf{l}_{machine}$	$\mathbf{l}_{st}$	$\mathbf{w}_{sy}$	$\mathbf{l}_{rt}$	$\mathbf{w}_{ry}$
[0.000 0.060 0.879 0.060]	249	23.9	31.1	33.9	30.3
7.Fitting the air-gap parameters in a machine with rectangular slots in the linear region					
[d1 d2 d3 d4]	$\mathbf{l}_{machine}$	$\mathbf{l}_{st}$	$\mathbf{w}_{sy}$	$\mathbf{l}_{rt}$	$\mathbf{w}_{ry}$
[0.202 0.0624 0.103 0.0698]	249	23.9	31.1	33.9	30.3
8.Fitting the air-gap parameters in a machine with rectangular slots considering the effect of saturation					
[d1 d2 d3 d4]	$\mathbf{l}_{machine}$	$\mathbf{l}_{st}$	$\mathbf{w}_{sy}$	$\mathbf{l}_{rt}$	$\mathbf{w}_{ry}$
[0.561 0.624 0.103 0.0698]	249	23.9	31.1	33.9	30.3
9.Fitting the air-gap parameters in a machine with rectangular slots , where the length of stator slots and width of stator yoke are optimized keeping the rotor linear					
[d1 d2 d3 d4]	$\mathbf{l}_{machine}$	$\mathbf{l}_{st}$	$\mathbf{w}_{sy}$	$\mathbf{l}_{rt}$	$\mathbf{w}_{ry}$
[0.289 0.122 0.293 0.295]	249	21.2	33.8	33.9	30.3

10.Fitting the air-gap parameters in a machine with rectangular slots , where the length of rotor slots and width of rotor yoke are optimized keeping the stator linear					
[d1 d2 d3 d4]	$\mathbf{l}_{machine}$	$\mathbf{l}_{st}$	$\mathbf{w}_{sy}$	$\mathbf{l}_{rt}$	$\mathbf{w}_{ry}$
[0.235 0.294 0.235 0.235]	249	23.9	31.1	42.7	21.5
11.Fitting the air-gap parameters in a machine with the original slots with rotor slots open , where the length of stator slots and width of stator yoke are optimized keeping the rotor linear.					
[d1 d2 d3 d4]	$\mathbf{l}_{machine}$	$\mathbf{l}_{st}$	$\mathbf{w}_{sy}$	$\mathbf{l}_{rt}$	$\mathbf{w}_{ry}$
[0.0003 0.333 0.659 0.006]	249	19.6	36.4	33.9	30.3
12.Fitting the air-gap parameters in a machine with the original slots with rotor slots open ,where the length of rotor slots and width of rotor yoke are optimized keeping the stator linear.					
[d1 d2 d3 d4]	$\mathbf{l}_{machine}$	$\mathbf{l}_{st}$	$\mathbf{w}_{sy}$	$\mathbf{l}_{rt}$	$\mathbf{w}_{ry}$
[0.017 0.949 0.017 0.017]	249	23.9	31.1	24.4	39.8
13.Fitting the air-gap parameters in a machine with the original slots with rotor slots open ,where the length of rotor slots,width of rotor yoke,length of stator slots and the width of stator yokes are optimized.					
[d1 d2 d3 d4]	$\mathbf{l}_{machine}$	$\mathbf{l}_{st}$	$\mathbf{w}_{sy}$	$\mathbf{l}_{rt}$	$\mathbf{w}_{ry}$
[0.114 0.019 0.856 0.010]	249	22	33	14.9	49.3

In Fig 8.9, the analytical function defined by the parameters [d1,d2,d3,d4] for defining the air-gap permeance is plotted for understanding each of the cases under consideration in Table 8.3.

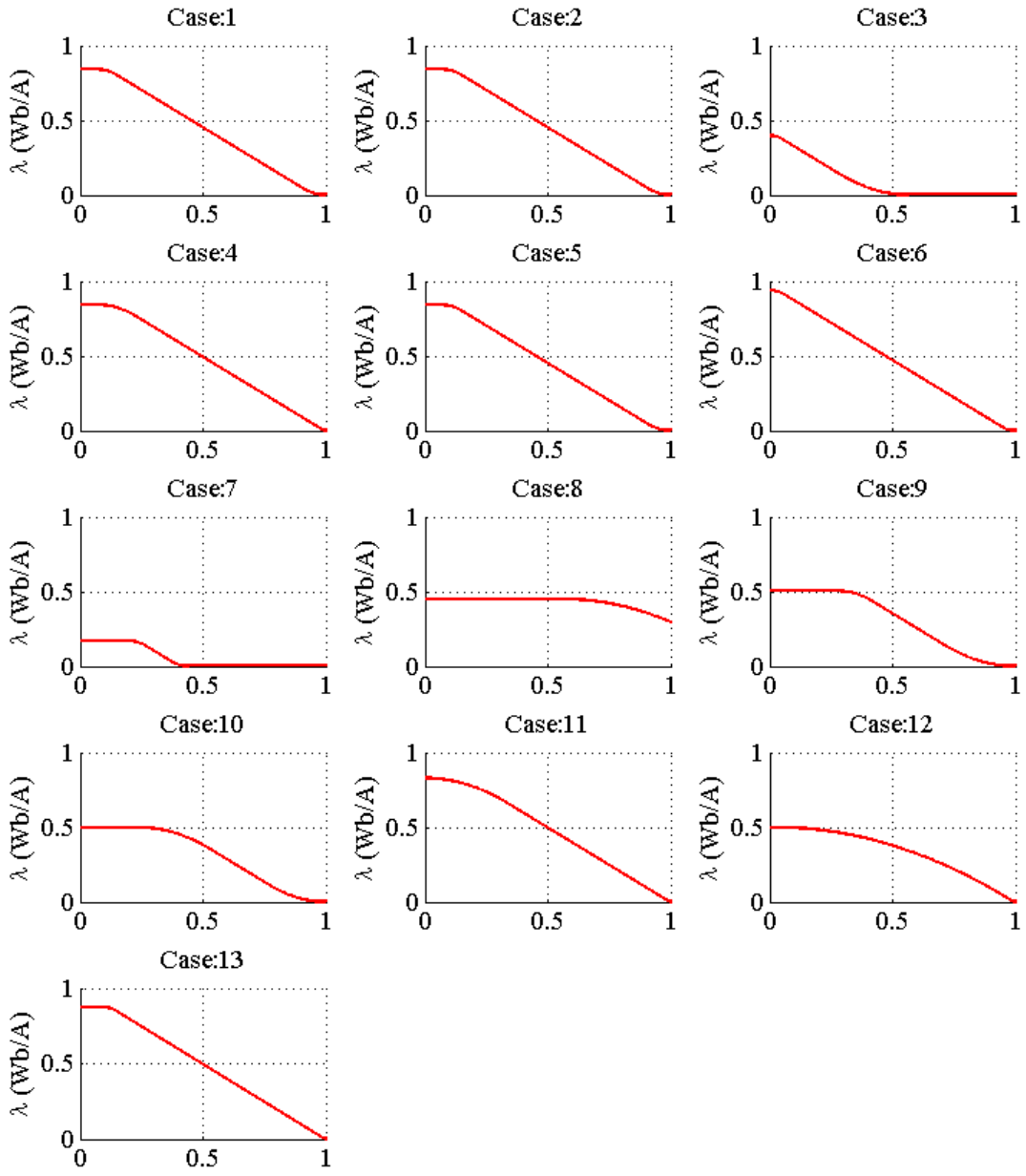

Figure 8.9: Permeance profile in the air-gap for all the cases under consideration